Lateral Hypothalamic GABAergic neurons encode and potentiate sucrose's palatability

Aketzali Garcia, Alam Coss, Jorge Luis-Islas, Liliana Puron-Sierra, Monica Luna, Miguel Villavicencio, Ranier Gutierrez*

Laboratory of Neurobiology of Appetite; Department of Pharmacology, CINVESTAV, 07360. Mexico City, Mexico.

***Ranier Gutierrez**
Email: ranier@cinvestav.mx
ORCID: https://orcid.org/0000-0002-9688-0289

LHA^{Vgat+} neurons, feeding circuits, palatability, sucrose

Author Contributions
A.G., A.C., J. LI., and R.G. designed research; A.G., A.C., J. LI., L.PS., and M.L. performed research; M.V. contributed unpublished analytic tools; A.G., A.C., J. LI., and R.G. analyzed data; all authors reviewed and approved manuscript; A.G. and R.G. wrote the paper.

This PDF file includes:
Main Text 6729
Methods 1980
Figures 1 to 7
Tables 0

Abstract

Overconsumption of calorie-dense palatable foods, especially those with added sugars, is a contributing factor in the obesity epidemic. Although previous studies in mice have shown that GABAergic LHA^{Vgat+} neurons evoke voracious eating, it is not known whether these neurons would be driving consumption by increasing palatability. Using optrode recordings, we measure sucrose's palatability while VGAT-ChR2 transgenic mice performed a brief access sucrose test. We found that a subpopulation of LHA^{Vgat+} neurons encodes palatability responses elicited by sucrose and that opto-stimulation of these neurons bias the intake towards the most palatable available tastant. In contrast, opto-self-stimulation of LHA^{Vgat+} neurons convey a rewarding signal capable of enhancing the hedonic value of proximal stimuli. We conclude that LHA^{Vgat+} neurons increase consumption by potentiating the palatability of the most proximal tastant available. These findings suggest that LHA GABAergic neurons could be a pharmacological target to modulate the palatability of caloric foods that produce obesity.

Impact Statement

Sucrose is attractive due to its sweet taste and positive palatability. LHA GABAergic neurons encode sucrose's palatability and act by increasing consumption of the most palatable and proximal tastant available.

Introduction

The Lateral Hypothalamic Area (LHA) been regarded as the “feeding center” since its lesion results in hypophagia and subsequent death (Anand and Brobeck, 1951; Teitelbaum and Epstein, 1962). It is part of a neural circuit related to eating and reward (Delgado and Anand, 1953; Olds and Milner, 1954) as rats are willing to press a lever to deliver electrical intra-cranial self-stimulation (ICSs), and if food is available, it also promotes feeding (Coons and Cruce, 1968; Delgado and Anand, 1953; Mendelson, 1967; Mogenson and Stevenson, 1967). Moreover, if a sweet tastant is available, the rate of electrical ICSs is further increased, whereas bitter compounds decreased ICS rates (Phillips and Mogenson, 1968; Poschel, 1968), suggesting an interaction between ICSs and taste palatability. In this regard, and because of its connections with different cortical and subcortical gustatory regions (Berk and Finkelstein, 1982; Berthoud and Münzberg, 2011; Simerly, 2004; Ter Horst and Luiten, 1987), the LHA is anatomically posed to processes and broadcast taste palatability information (Berridge and Valenstein, 1991; Ferssiwi et al., 1987). Pioneering electrophysiological studies have recorded in LHA gustatory responses (Schwartzbaum, 1988a; Yamamoto et al., 1989), and one recent study uncovered two functional populations of LHA neurons: one that was activated by palatable tastants, e.g., sucrose, and the other by aversive tastants, like quinine (Li et al., 2013). However, the genetic identity of the LHA cell-type(s) involved in processing palatability-related information remains elusive, and to unveil their identity is a goal of this study.

Currently, the LHA is viewed as a hub of various cell-types (Stuber and Wise, 2016) grossly divided into two larger populations related to feeding: the glutamatergic ($LHA^{Vglut2+}$) and

GABAergic neurons (LHA^{Vgat+}) (Gutierrez et al., 2020). Activation of $LHA^{Vglut2+}$ neurons leads to reduced food intake and is aversive (Jennings et al., 2013). In contrast, stimulation of LHA^{Vgat+} neurons is rewarding and produces voracious eating of both foods with nutritional value (Jennings et al., 2015; Navarro et al., 2016) as well as those without calories or even gnawing behavior towards irrelevant biological stimulus (Navarro et al., 2016). Moreover, LHA^{Vgat+} neurons enhance the salience of the nearest stimuli and induce reward via stimulation of their projections to the ventral tegmental area (VTA) (Nieh et al., 2016), whereas the evoke feeding is mediated by modulation of terminals reaching a region adjacent to the locus coeruleus (Marino et al., 2020). Contrary, inhibition of GABAergic LHA^{Vgat+} cell somas is aversive and stops feeding (Jennings et al., 2015; Navarro et al., 2016). However, the role of LHA^{Vgat+} neurons in processing sucrose's palatability remains to be determined.

In this study, we identified a new role of LHA^{Vgat+} neurons in encoding and enhancing sucrose's palatability. We found that LHA GABAergic neurons act to enhance the consumption of the most palatable and proximal tastant available. They accomplish this by potentiating the palatability of nearby and appetitive gustatory stimuli. For aversive stimuli, the effect of these neurons is different. In a single bottle test, we found that water deprivation increased the tolerance for bitter compounds and gated a widow of opportunity where activation of GABAergic neurons is sufficient to temporarily reassign the negative hedonic value of quinine and to promotes its intake. Nevertheless, in a three-options preference test, these neurons failed to develop a preference to quinine when sucrose was available. Moreover, optogenetic activation of LHA^{Vgat+} neurons evoked many hallmark behaviors resembling those seen in LHA electrical stimulation. In this regard, and consistent with their positive role in palatability, our results could explain why electrical ICSs are further facilitated by the presence of sweet solutions (Phillips and Mogenson, 1968; Poschel, 1968). We also

found that LHA^{Vgat+} neurons are the common neural substrate for both reward and feeding since after repeated self-stimulation, the more the VGAT-ChR2 mice opto-self-stimulated, the stronger the laser-induced licking they exhibited. In sum, we conclude that GABAergic LHA^{Vgat+} neurons combine stimulus-proximity and palatability related information to enhance the palatability of nearby energy-rich foods.

Results

Initially, we determined the optimal stimulation parameters to activate LHA GABAergic neurons. This was accomplished by implanting an optrode in naïve mice that constitutively expressed ChR2 in GABAergic neurons expressing the gene for the vesicular γ-aminobutyric acid transporter (VGAT-ChR2 mice) (Zhao et al., 2011) (Figure 1—figure supplement 1A-B). We found that a laser stimulation of 50 Hz (10 ms width) evoked the strongest LHA neuronal responses (Figure 1—figure supplement 1D-H) (Gigante et al., 2016). Unless otherwise mentioned, this frequency was used in all subsequent experiments.

LHA neurons encode sucrose's palatability

In rats, previous electrophysiological studies suggest that ensembles of LHA neurons process palatability related information (Li et al., 2013; Norgren, 1970; Schwartzbaum, 1988b; Yamamoto et al., 1989). Based on these results, we then asked whether LHA neurons could provide information about sucrose's palatability by using a behavioral task with only palatable stimuli (i.e., artificial saliva (AS), water, sucrose 3 wt%, and sucrose 18 wt%). We operationally defined sucrose's palatability as the enhancement of hedonically positive oromotor responses triggered by increasing concentrations of sucrose (Berridge and Grill, 1983; Spector et al., 1998; Villavicencio et al., 2018). Specifically, oromotor responses include an increase in the lick rate or bout size. Thus, this definition of palatability

should not be confused with a conscious hedonic feeling of pleasant taste that humans experience (Grill and Berridge KC, 1985; Sclafani, 1991). To this end, taste responses were recorded from a total of 284 LHA neurons, while VGAT-ChR2 mice performed a brief access test (Figure 1A). To uncover palatability-responsive neurons, we analyzed neuronal activity using a previously described “best-window analysis” (Villavicencio et al., 2018). Briefly, this strategy detects the optimal interval (brown shadow Figure 1B), where the firing rate best correlates with the sucrose’s palatability index (PI) computed as the average lick rate, in a session by session basis, evoked by each gustatory stimulus in the Reward epoch (Figure 1C). Figure 1B depicts the responses of two representative LHA neurons: as expected, we found one whose activity increased as the sucrose concentration increased (positive Pearson’s correlation, r = 0.87; Figure 1B *left*), and another that was negatively associated with palatability oromotor responses evoked by sucrose (r = -0.64; Figure 1B *right).* Figure 1D shows the normalized activity exhibiting either positive (59/284 neurons, 21%) or negative correlations (76/284, 27%) with the PI. Thus, these data confirmed that the LHA mice’s neurons exhibit palatability-related responses, and this activity can be either correlated or anti-correlated with the sucrose solution’s PI.

Dynamic tracking of palatability throughout a session

Having demonstrated that LHA neurons could encode sucrose’s palatability, we then explored whether LHA palatability-related neurons can dynamically adjust their responses to track the changes in sucrose’s palatability throughout the session when the animals would approach satiation. We found that the lick rate declined across the session as a function of sucrose’s palatability (Figure 1—figure supplement 2A [RM ANOVA, main effect of stimuli $F_{(3, 402)} = 163.7$, $p < 0.0001$,effect of time $F_{(9, 1206)} = 100.4$, $p < 0.0001$), and significant interaction stimuli by time $F_{(27, 3618)} = 16.54$, $p < 0.0001$]). Briefly, early in the session, animals

licked more for all stimuli, but as the session progressed, the lick rate declined especially for AS and water but not for sucrose (3% and 18%), indicating that they tracked palatability responses rather than satiety (Figure 1—figure supplement 2A). Similar to our previous work in the Nucleus Accumbens Shell (NAcSh) (Villavicencio et al., 2018), we also found that the LHA neuron's firing rate either increasing or decreasing neurons adjust their activity throughout the session to reflect sucrose's palatability (Figure 1—figure supplement 2B). These data indicate that as the animals approach satiety, the responses of the Palatability related-neurons tracked the rapid decline in the lick rate throughout the session mainly for the two lower stimuli (i.e., AS and water) but not for the higher sucrose-concentration (sucrose 3% and 18%), suggesting these neurons are tracking palatability, rather than internal sates.

A subpopulation of opto-identified LHA^{Vgat+} neurons encodes sucrose's palatability

To identify LHA^{Vgat+} neurons from our recordings, we opto-stimulated the same mice recorded in the brief access test seen in Figure 1. Importantly, we verify the stability of the waveforms across both tasks (BAT and Optotagging), and we only included in analysis single units with stable waveforms (Figure 1—figure supplement 3). Figure 2A displays the normalized (Z-score) activity of 48% (137/284) of laser-activated neurons (see Material and Methods). Since these neurons may include ChR2 expressing cells and other LHA neurons modulated by indirect polysynaptic feedback of afferent fibers from other areas in the brain (Nieh et al., 2015), we decided to name them putative LHA^{Vgat} (pLHA^{Vgat}) neurons. Note that, pLHA^{Vgat} neurons comprise the ensemble recruited by the optogenetic stimulation of LHA GABAergic neurons, suggesting they convey similar information. Therefore, we next evaluated whether pLHA^{Vgat} neurons are correlated with sucrose's palatability. In total 50% (69/137) of laser-activated neurons exhibited responses that were significantly palatability

related; specifically, 34% showed a positive correlation (46 out of 137), whereas 17% (23 out of 137) had a negative correlation with sucrose's palatability (Figure 2B, Positive vs. Negative chi-square test $_{(1, 274)}$ = 10.25, $p < 0.01$). Figure 2C shows the population activity of pLHA^{Vgat} neurons with either a positive or negative correlation with the PI. To confirm the identity of LHA^{Vgat+} neurons, we searched for neurons in which a brief pulse of light-evoked an action potential with an early latency (< 15 ms), that would reflect the expression of ChR2 (Buonomano, 2003). Thus, from the pLHA^{Vgat} population, in total, 52 % (71 / 137) neurons exhibited an early response to blue light (Figure 2E-F), suggesting that these pLHA^{Vgat} neurons were LHA^{Vgat+} neurons. We found that 31% of LHA^{Vgat+} neurons correlated positively with sucrose's palatability (22/71), and 24% were anticorrelated (17/71) (Figure 2G, Positive vs. Negative; n.s.). The LHA^{Vgat+} neuronal responses with positive (yellow) and negative (purple) correlations with lick-related palatability responses (red) are seen in Figure 2H. Hence, over half of the identified LHA^{Vgat+} neurons, 55% (39/ 71), were involved in encoding sucrose's palatability. The remainder of 45% of LHA^{Vgat+} neurons were unmodulated by sucrose. In agreement, with the idea that the LHA^{Vgat+} population contains many subpopulations with different functional responses, with at least one ensemble responding to appetitive (approach) and others to consummatory behaviors (Jennings et al., 2015).

Non-LHA^{Vgat} neurons negatively encode sucrose's palatability

In contrast, we found that 25% of LHA neurons exhibited a laser-induced inhibition (70/284, non-LHA^{Vgat} neurons, Figure 2—figure supplement 1A), and the remaining 27% (77/284) were unmodulated during blue light stimulation (Figure 2—figure supplement 1A, black trace). Unlike pLHA^{Vgat} neurons, only 7% (5 out of 70) of the non-LHA^{Vgat} neurons showed a positive correlation, whereas the vast majority 36% (25 out of 70) had a negative correlation with sucrose's palatability (Figure 2—figure supplement 1B, Positive vs. Negative chi-square test $_{(1, 140)}$ = 16.97, $p < 0.0001$). These results suggest that non- LHA^{Vgat} neurons (perhaps

glutamatergic Vglut2 neurons) preferentially encode sucrose's palatability with negative correlations (Figure 2—figure supplement 1D, Positive vs. Negative chi-square test $_{(1, 135)}$ = 11.46, $p < 0.001$).

LHA GABAergic neurons had a bias to encode sucrose's palatability by increasing firing rates

From the LHA neurons encoding sucrose's palatability, we next wondered whether LHA GABAergic neurons were biased towards positive correlations with sucrose's palatability. Remarkably, from all positive palatability-responsive neurons recorded in the LHA (n = 59, see Figure 1D), more than 78% (46/59) belonged to the pLHA^{Vgat} (Figure 2D). In contrast, only 30% (23/76) of pLHA^{Vgat} neurons were Negative palatability related (Figure 2D, Positive vs. Negative chi-square test $_{(1, 135)}$ = 30.25, $p < 0.0001$). A similar but non-significant trend was observed for the opto-identified LHA^{Vgat+} neurons. That is, 37% (22/59) of LHA^{Vgat+} neurons belonged to the Positive palatability-related population, whereas only 22% (17/76) were Negative palatability-related neurons (Figure 2I, Positive vs. Negative; n.s). Altogether, these data suggest that LHA^{Vgat+} neurons tend to encode sucrose's palatability in a positive, rather than in a negative manner.

Activation of LHA^{Vgat+} neurons drives sucrose intake

If LHA GABAergic neurons preferentially encode sucrose's palatability by increasing firing rates, their optogenetic stimulation should promote increased sucrose intake. To characterize their impact on sucrose intake, we used an open loop optogenetic stimulation involving 5 min blocks with laser and no-laser stimulation, while naïve VGAT-ChR2 mice had *ad lib* access to a sipper filled with sucrose 10% (Figure 3*A*). We analyzed the intake as a function of laser frequency and found that in the first three blocks with laser, 50 Hz

stimulation induced a significant increase in sucrose intake (Figure 3B; Blocks 2, 4, and 6) compared with the previous blocks of no-laser (Figure 3*B;* $p < 0.001$; Blocks 1, 3, and 5). Figure 3*C* shows a raster plot for licking responses of a representative open loop session. At 50 Hz, we found that feeding (licking) was elicited within a 0.72 s ± 0.03 latency from laser onset, and it abruptly stopped (0.27 s ± 0.1) after laser offset (see blue dash rectangles). VGAT-ChR2 mice exhibited an increase in the laser-bound feeding index (number of licks in a 2.5 s window from laser onset divided by total licks in the session; hereafter named laser-bound feeding) as the laser frequency increased (Figure 3*D;* two-way ANOVA, group by frequency interaction; $F_{(5, 36)} = 12.86$, $p < 0.0001$). Thus, to induce sucrose intake, a subset of LHA^{Vgat+} neurons requires continued activation. Our data then confirmed that 50 Hz is the best stimulation frequency to drive both neuronal responses and sucrose intake.

LHA^{Vgat+} neurons do not induce a persistent hunger state

A previous study showed that brief optogenetic stimulation of “hunger-inducing” AgRP neurons before food availability promotes consummatory behavior that persists for several minutes in the absence of continued AgRP neuron activation (Burnett et al., 2016; Chen et al., 2016). Based on this study, we tested whether the pre-stimulation of LHA^{Vgat+} neurons could evoke a similar hunger state. Unlike AgRP neurons (Burnett et al., 2016; Chen et al., 2016), pre-stimulation of LHA^{Vgat+} neurons failed to evoke and sustain subsequent sucrose intake (Figure 3—figure supplement 1). Our results suggest that feeding occurs while LHA^{Vgat+} neurons are active, but they do not induce a persistent hunger state as AgRP neurons do.

Open loop activation of LHA^{Vgat+} neurons drives intake of the highest sucrose concentration available

To test whether activation of LHA^{Vgat+} neurons promotes the intake of the most palatable available stimuli, a group of naïve WT and VGAT-ChR2 mice was opto-stimulated in an open loop protocol, with access to three adjacent ports containing water, sucrose 3%, or sucrose 18% (Figure 4A). As expected, both WT and VGAT-ChR2 mice preferred sucrose 18% over water and sucrose 3% (Figure 4B, [WT: two-way ANOVA main effect tastants; $F_{(2, 1560)} = 543.3$, $p < 0.0001$; VGAT-ChR2: $F_{(2, 3144)} = 983$, $p < 0.0001$]). However, we found that during laser stimulation sated VGAT-ChR2 mice increased the intake of 18% sucrose but mainly during the laser-activated blocks compared with controls (Figure 4B-*right*, [two-way ANOVA group by laser block interaction $F_{(14, 3144)} = 61.32$, $p < 0.0001$]) and rarely licked in the absence of stimulation. In this regard, VGAT-ChR2 mice seem to counteract the evoked sucrose intake by voluntarily restraining consumption in no-laser blocks (Blocks numbers 3, 5, and 7), resulting in no significant differences between groups in the total intake of 18% sucrose (Figure 4C, unpaired Student's t-test, $t_{(196)} = 1.512$, $p = 0.1320$). An across days analysis revealed that the evoked 18% sucrose intake began from the first stimulation day (Figure 4D [RM ANOVA laser blocks, $F_{(1, 22)} = 64.64$, $p < 0.0001$]), although sucrose consumption ramps up across days (Figure 4D [RM ANOVA main effect days, $F_{(10, 220)} = 2.169$, $p < 0.05$]). This suggests that LHA^{Vgat+} neurons, rather than inducing hunger *per se*, induced a learning process that potentiates the intake of the most palatable stimulus and confines consumption mainly in the presence of opto-stimulation.

The small increase in water and sucrose 3% intake observed during opto-stimulation of LHA^{Vgat+} neurons could be explained by random stimulation near those tastants (Figure 4B *right panel*). Accordingly, we found in laser blocks 2, 4, and 6, a significant increase in water and sucrose 3% in the VGAT-ChR2 mice compared with the WT mice that completely neglected those tastants (Figure 4B, ^ $p < 0.05$ for sucrose 3%; † $p < 0.05$ for water). We hypothesize that this additional intake can be attributed to trials where the laser-activation

occurred near these less palatable stimuli. A detailed videography analysis found exactly that (Figure 4—figure supplement 1A-B). When opto-stimulation occurred in a distance minor to 50 pixels (approximately 3 cm, see Materials and Methods) relative to water or sucrose 3% ports, the licking probability increased significantly after opto-stimulation (Figure 4—figure supplement 1B). The angle of the head was less informative (Figure 4—figure supplement 1C and 1D). Conversely and since mice are naturally attracted to the most palatable tastant, they spent more time near the lateral port with 18% sucrose, increasing their overconsumption (Figure 4—figure supplement 1C, Video1). We observed that for the sucrose 18% port, even when the mouse position was twice as far (i.e., 6 cm) from sucrose 18% port, the licking probability increased significantly. These data are consistent with a study showing that opto-stimulation of LHA^{Vgat+} neurons promotes the intake of the nearest stimulus (Nieh et al., 2016) but further demonstrates that the most palatable stimulus have nearly twice the distance of attraction than the other less palatable options.

Open loop activation of LHA^{Vgat+} neurons also increases the time spent and drives intake of the most palatable solid food available

We also explored whether LHA GABA neurons could induce the intake of the most palatable solid food available. Thus, using an open loop protocol, we opto-stimulate these neurons while mice choose among different solid foods, we found that optogenetic activation of LHA^{Vgat+} neurons increased the time spent near the most palatable food available. Mice spent more time near the high-fat diet than the granulated sugar cube or the chow food pellet (Figure 4—figure supplement 2 and Video 2). When mice could choose between both a sugar cube and a chow pellet, activation of these neurons increased the consumption of sugar cube over chow (Figure 4—figure supplement 3 and Video 3). Our data suggest that

open loop stimulation of LHA GABAergic neurons promotes the intake of the most palatable food available.

Closed-loop stimulation of LHA^{Vgat+} neurons drives intake of the nearest appetitive stimuli

To further test the idea that LHA^{Vgat+} neurons could induce preference to a proximal (but less palatable) stimulus over a distal one with higher hedonic value, we used a closed-loop stimulation protocol. That is, the same mice were photostimulated, but here the laser was triggered by each head entry in the central port (i.e., opto-self-stimulation). This closed-loop configuration guarantees that stimulation only occurs proximal to water, the least palatable stimulus of the three in the box (Figure 5*A-right*). We found that activation of LHA^{Vgat+} neurons is rewarding since transgenic mice visited the central port significantly more and performed more opto-self-stimulations than the WT mice (Figure 5B, unpaired Student's t-test, $t_{(196)} = 12$, $p < 0.0001$). Surprisingly, the total number of licks in the session seen in Figure 5C shows that during closed-loop stimulation, the VGAT-ChR2 mice explored and consumed more water than the WT mice. Note that in both (open loop and closed-loop) protocols, the WT and VGAT-ChR2 mice exhibited, at the end of the session, a similar number of licks for 18 wt% sucrose (Figure 5C [two-way ANOVA group by protocol interaction $F_{(1, 391)} = 1.854$, $p = 0.1741$]). That is, the total licks for sucrose 18% were not significantly different between groups, suggesting that these neurons do not interfere with the overall attractiveness of sucrose. In contrast, and by counting the number of licks given when the laser was turned on (in a 2.5 s window from laser onset- see Figure 5D), we uncovered a striking change in preference. As noted, in the open loop, the VGAT-ChR2 mice exhibited a higher preference for sucrose 18 wt% over both sucrose 3 wt% and water. In contrast, in the closed-loop protocol, the same transgenic mice now consumed more water compared with WT ($p < 0.0001$), and the consumption of water was about the same

as sucrose 18% (p = 0.8729, n.s.; Figure 5D). Thus, LHA^{Vgat+} neurons could promote water intake, but only when it is the nearest stimulus. The sucrose preference index (Figure 5E) showed that during the open loop all VGAT-ChR2 mice preferred sucrose 18% over water (Figure 5E; values > 0.5 and near to 1) whereas in the closed-loop protocol, when water was the nearest stimulus, most mice (n = 9 out of 12), significantly diminished their sucrose preference (Figure 5E, see the drop in preference index; paired Student's t-test, $t_{(58)} = 7.98$, $p < 0.0001$). From these 9 animals, 6 exhibited a higher preference for water over sucrose 18% (Preference index values < 0.5; Video 4). Figure 5F shows the location of fiber tips color-coded for each VGAT-ChR2 mice plotted in Figure 5E. However, the location of fibers does not explain the variability in preference. Perhaps variability is due to different behavioral strategies used by each mouse. Nevertheless, the large variability in the drop of sucrose's preference resembled that found with the sweet-induced facilitation by electrical ICSs (Poschel, 1968). In sum, these data suggest that LHA^{Vgat+} neurons drive consummatory behavior by integrating the proximity and the hedonic value of the stimulus.

After repeated stimulation, the correlation between laser-bound feeding and self-stimulation strengthens

Previous studies have shown that after repeated LHA bulk stimulation (either electrically or with optogenetic targeting all cell-types together), subjects switched from exhibiting stimulus-bound feeding to only self-stimulating, indicating that LHA evoked feeding and reward could represent two distinct processes (Gigante et al., 2016; Urstadt and Berridge, 2020). Consequently, we explored whether laser-bound feeding changed after repeated optogenetic stimulation. In contrast to previous studies, we observed that laser-bound feeding induced by LHA^{Vgat+} neurons strengthened across sessions (Figure 5—figure supplement 1A , First 3 days: r = 0.12, p = 0.69; Last 5 stimulation days: r = 0.63, p < 0.05)

and after repeated stimulation, both opto-self-stimulation and laser-bound feeding exhibited a robust correlation (Figure 5—figure supplement 1B, First 3 days: $r = 0.42$, $p = 0.16$; Last 5 days: $r = 0.61$, $p < 0.05$), suggesting that LHA evoked-feeding (licking) involves a learning process (Sharpe et al., 2017) and that LHA GABAergic neurons are a common neural substrate for feeding and reward.

The "stimulus-proximity effect" is not restricted to liquid tastants, and it also occurs with chocolate and chow pellets

The "proximity effect" evoked by LHA^{Vgat+} neurons was not restricted to liquid tastants. In a real-time place preference arena, when chocolate pellets or chow food were the designated foods to be near opto-self-stimulation of LHA^{Vgat+} neurons, mice also increased the time spent near those foods (Figure 5—figure supplement 2B; Video 5) and their intake (Figure 5—figure supplement 1C). Thus, LHA GABAergic neurons reinforced the approach and exploration to any, if not the most appetitive stimuli, that happened to be proximal to the opto-stimulation.

LHA^{Vgat+} neurons activation is rewarding

In the same WT and VGAT-ChR2 mice tested in the closed-loop configuration seen in Figure 5, we went on to show that mice visited the central water-port to opto-self-stimulate. To do this, we performed an extinction session with the laser disconnected (Figure 6A). We observed a rapid decrease in the number of opto-self-stimulations (Figure 6B; Extinction phase, gray shadow). As expected, self-stimulation rapidly recovered when the laser was turned "on" again (Figure 6, see water after extinction). Thus, LHA^{Vgat+} neurons convey a hedonically positive, rewarding signal (Jennings et al., 2015).

LHA^{Vgat+} neurons also promote licking an empty sipper

A previous study demonstrated that chemogenetic activation of LHA^{Vgat+} neurons increased gnawing to non-edible cork (Navarro et al., 2016). In the absence of other stimuli but cork, we also observed in some mice gnawing behavior, although we did not systematically study stereotypy (see Video 6). Instead, we further explored this idea by replacing water, in the central port, with an empty sipper (Figure 6, Empty sipper). Transgenic mice continued opto-self-stimulating at the same pace as if water were still present in the central port. LHA^{Vgat+} stimulation evoked licking an empty sipper compared with WT mice (Figure 6C, unpaired Student's t-test, $t_{(40)}=2.532$, $p < 0.05$). Thus, LHA^{Vgat+} neurons evoke an imminent urge to express consummatory behavior even in the form of dry licking an empty sipper, a non-biological relevant stimulus. This effect is perhaps mediated by an increase in the rewarding value of appetitive oromotor responses *per se*.

When sucrose is available, activation of LHA^{Vgat+} neurons neither promotes liquid intake of an aversive bitter tastant nor tolerance of punishment, but it further increases sucrose consumption

To explore whether the "stimulus-proximity effect" also applied to aversive stimuli, we replaced the central stimulus (water) with aversive stimuli, including quinine or airpuffs (Figure 6*A*). Upon quinine presentation, the number of licks given in central port sharply fell (Figure 6C, green), but transgenic mice continued to self-stimulate and go to the lateral port to lick for sucrose 18% (Figure 6D, green). Also, with a new group of naïve mice, we corroborated if photostimulation of LHA^{Vgat+} neurons induced quinine intake when it was the only option. Surprisingly, we found that activation of LHA^{Vgat+} neurons promoted a higher

quinine intake when transgenic mice were water-deprived (Figure 6—figure supplement 1B, unpaired Student's t-test, $t_{(5)} = 5.821$, $p < 0.0001$). However, in sated mice, it did not affect quinine intake relative to WT (Figure 6—figure supplement 1A), suggesting that activation of LHA^{Vgat+} neurons is sufficient to increase the palatability of bitter tastants but only during water deprivation.

During the airpuff delivery phase (Figure 6D, dark gray), we obtained similar results as in quinine stimulation. Next, we required the animal to lick, at least once, the central sipper to trigger opto-stimulation (thus making the airpuffs unavoidable). Under this condition, transgenic mice completely stopped self-stimulation (Figure 6B, cyan) and aborted 18% sucrose intake from the lateral port (Figure 6D, cyan). These results suggest that, in sated mice, LHA^{Vgat+} neurons did not induce quinine intake or increase tolerance to airpuffs.

Finally, we explored whether proximity to the most palatable tastant further facilitated its overconsumption. Thus, we exchanged the position of water and sucrose 18%. When sucrose 18% was delivered in the central port, transgenic mice greatly overconsumed it (Figure 6C, pink). The intake of sucrose 18% was higher than for all the other tastants tested previously ($p < 0.0001$). We found that regardless of homeostatic needs, activation of these neurons increased sucrose 18% intake relative from WT mice (Figure 6—figure supplement 1C-D). These results collectively suggest that activation of LHA^{Vgat+} neurons is rewarding and promotes increased consumption of the nearest stimulus even if it is not the most palatable (e.g., water and empty sipper). If the nearest stimulus happens to be the most palatable (i.e., sucrose 18%), then LHA GABA neurons further facilitated its consumption.

Activation of LHA^{Vgat+} neurons enhances palatability

We next explored whether, at equal stimulus distance, activation of these neurons could enhance palatability responses. To do this, in a new group of water-deprived mice, we employed a brief access test again. In this task, we delivered gustatory stimuli water, sucrose 3%, and sucrose 18% from the same sipper tube, but in different trials. Figure 7*A* displays the structure of a trial (same conventions as in Figure 1). We found that WT mice increased their licking rate as a function of sucrose's concentration (Figure 7B, *left panel*). In contrast, during the 2 s of laser stimulation, the VGAT-ChR2 mice exhibited a greater lick rate for all three tastants. However, after the laser was turned "off," these mice abruptly stopped licking for water and sucrose 3% (Figure 7*B, right panel*) compared with the WT group.

Moreover, when stimulation was paired with water trials, transgenic mice increased their lick rate, but it was selective to water (Figure 7C; arrow), even surpassing licking responses evoked by the most palatable sucrose 18%. A similar enhancement of oromotor responses was observed by pairing sucrose 3% trials with LHA^{Vgat+} opto-self-stimulation (Figure 7D, pink). Likewise, the laser-bound feeding (licking rate) was strongest when sucrose 18% was paired with optogenetic stimulation (Figure 7E, red, see arrows).

Finally, we show that palatability responses could be artificially extended as long as LHA^{Vgat+} neurons were continuously activated. For this, we photostimulated them for up to 7 s. We observed a similar enhancement pattern, maintained for the duration of opto-stimulation (see Figure 7F-I see arrows), suggesting that LHA^{Vgat+} neurons can adjust the enhancement of oromotor palatability responses by simply sustaining its neuronal activity. We verified that using optrode recordings, that 7 s optogenetic stimulation produces sustained LHA^{Vgat+} neuronal responses (Figure 7—figure supplement 1). Moreover, transgenic mice did not merely use the light as a cue to guide behavior since laser-stimulation with a mock optic fiber failed to increase licking (Figure 7—figure supplement 2). In sum, our data demonstrate

that activation of LHA^{Vgat+} neurons triggers a reinforcing signal that amplifies the positive hedonic value of proximal stimuli, promoting overconsumption.

Discussion

LHA has historically been viewed as a critical center for feeding (Anand and Brobeck, 1951; Delgado and Anand, 1953; Teitelbaum and Epstein, 1962), although it also processes sucrose's palatability related information (Li et al., 2013; Norgren, 1970; Ono et al., 1986). In addition to caloric value, sucrose's palatability is the affective or hedonic attribute of sweetness that determines whether to like it. In rodents, it can be measured by the increase in the lick rate induced by stimulating the tongue with ascending sucrose's concentrations (Spector et al., 1998; Villavicencio et al., 2018). Despite the importance of palatability to promote overconsumption, the specific LHA cell-type(s) identity involved in processing sucrose's palatability has remained elusive. Our results demonstrated that a subpopulation of LHA^{Vgat+} GABAergic neurons encodes sucrose's palatability, by exhibiting two opposite modulatory patterns, either a positive or negative correlation with the palatability index, with a bias towards a positive correlation. Furthermore, opto-stimulation of LHA^{Vgat+} cell somas promoted approach and intake of the most salient available and palatable tastant. In contrast, opto-self-stimulation promoted increased liquid intake of the less-attractive and proximal stimuli, despite having more palatable but distal tastants available. These findings show that LHA^{Vgat+} neurons compute and/or combine, at least, two types of information: one related to stimulus proximity and the other to palatability that results in enhancing stimulus-saliency (Nieh et al., 2016). More important, these data uncovered a new function of LHA^{Vgat+} neurons as physiological potentiators of sucrose's palatability and suggested that these neurons are potential pharmacological targets that can modulate food's palatability.

Previous work has shown that activation of LHA^{Vgat+} neurons is rewarding, induces voracious eating (Jennings et al., 2015; Navarro et al., 2016), and promotes interaction of the nearest stimuli (either objects or another mouse) (Nieh et al., 2016) suggesting that they play a role in multiple motivated behaviors. However, it is also known that LHA connects and receives direct inputs from multiple cortical and subcortical gustatory regions (Berk and Finkelstein, 1982; Berthoud and Münzberg, 2011; Rolls, 2015; Simerly, 2004; Ter Horst and Luiten, 1987), and some electrophysiological studies report that LHA neurons respond to gustatory stimuli –in particular to tastant palatability (Karádi et al., 1992; Norgren, 1970; Ono et al., 1986; Schwartzbaum, 1988a; Yamamoto et al., 1989). As noted, in rodents, palatability is operationally defined as the enhancement of hedonically positive oromotor responses (Berridge and Grill, 1983; Spector et al., 1998). In agreement with this definition, we found that LHA palatability related-neurons tracked licking oromotor-related responses by increasing or decreasing their activity in a sucrose-concentration dependent manner. Also, across the course of the session LHA neurons tracked the sucrose's palatability rather than satiety/hunger signals. We then showed that LHA^{Vgat+} neurons could function as enhancers of sucrose's palatability. Also, optogenetic activation of these neurons can even enhance the palatability of a neutral stimulus (water if it is the nearest stimuli). We found an increased lick rate for water during activation of these neurons as if the animal were sampling a high sucrose concentration. Besides, their activation promotes the intake of liquid sucrose (or solid granulated sugar cube). These neurons also induce intake of other more palatable stimuli like high-fat pellets (Figure 4—figure supplement 2), similar to other GABAergic neurons but in zona incerta (Zhang and van den Pol, 2017). It is tempting to propose that LHA GABAergic neurons could mediate the supra-additive effects of combining fats and carbohydrates such as sucrose (DiFeliceantonio et al., 2018), but this remains to be experimentally tested.

Optogenetic stimulation of LHA GABAergic neurons can induce voracious eating (Jennings et al., 2015), yet unlike AgRP neurons (Chen et al., 2016), it has become clear that these neurons are not directly involved in evoking hunger (Burnett et al., 2016; Marino et al., 2020; Navarro et al., 2016). We found that LHA^{Vgat+} neurons, rather than inducing a hunger state *per se*, convey a positive valence signal that combines stimulus-proximity and palatability related information. These findings are in agreement with the idea that these neurons enhance the saliency of nearby hedonically positive stimuli, whether those stimuli are sapid chemicals, as we show, or social cues, as in the approach behavior towards juvenile or female intruders and new objects (Nieh et al., 2016).

It is also important to highlight that opto-self-activation of LHA^{Vgat+} neurons resembles many hallmark behaviors evoked by LHA electrical stimulation. In particular, our data rationalized why, at low-intensity electrical currents, lever pressing to deliver ICSs only occurs if food (or sucrose) is in close proximity (Coons and Cruce, 1968; Mendelson, 1967; Valenstein et al., 1968; Valenstein and Phillips, 1970). Moreover, and consistent with its role in enhancing sucrose's palatability, activation of LHA^{Vgat+} neurons could explain the long-standing and puzzling result of why sweet tastants further potentiate the rate of LHA electrical ICSs (Poschel, 1968). We concluded that LHA^{Vgat+} neurons (or specifically a subpopulation of these LHA^{Vgat+} neurons) could account for many, if not all, of these electrically induced phenomena. That said, we also found differences between unspecific LHA stimulation and our targeted LHA^{Vgat+} stimulation. Unlike electrical LHA stimulation, we found that the laser-bound feeding was observed in all tested VGAT-ChR2 mice (n = 25, from Figure 3-7 and Figure 6—figure supplement 1). This is, in contrast, to the high variability found in rats exhibiting LHA electrically-induced feeding (for example, one study reported that only 12 of 34 rats showed stimulus-bound feeding (Valenstein and Cox, 1970). Similarly, a large

variability was observed when unspecific bulk optogenetic stimulation activated *all* cell-types found in LHA, simultaneously (Urstadt and Berridge, 2020). These studies reported that after repeated LHA stimulation (either electrically or with optogenetics), some subjects switched from exhibiting stimulus bound feeding to only self-stimulating, suggesting that these two processes were flexible and not correlated (Gigante et al., 2016; Urstadt and Berridge, 2020). In contrast, we found that repeated stimulation of LHA^{Vgat+} neurons increases laser-induced feeding (licking). Likewise, the correlation between optogenetic self-stimulation and laser-bound feeding increases across stimulation days (Figure 5—figure supplement 1). That is, the more the animals self-stimulated, the stronger the evoked laser-bound licking was. Thus, LHA^{Vgat+} neurons are the common neural substrate for evoking both feeding and reward. Though, it was recently shown that they do it by using two projection pathways; reward via VTA and feeding via peri-Locus Coeruleus nuclei (Marino et al., 2020).

Given than LHA is involved in reward and aversion (Ono et al., 1986), we next tested whether LHA^{Vgat+} neurons could promote the intake of bitter tastants. We found that opto-stimulation of LHA^{Vgat+} neurons failed to promote quinine intake, a bitter tastant, or tolerance of an aversive airpuff when sucrose was also available. Thus, these neurons play a minimal role in increasing the preference for a proximal but aversive stimulus over distal sucrose. Furthermore, in sated mice and using a single bottle test, these neurons also failed to increase quinine intake. Unexpectedly, during water deprivation, a copious quinine consumption was observed. These results agree with previous findings that chemogenetic inhibition of LHA^{Vgat+} neurons did not alter the rejection responses induced by quinine. Thus, in sated mice, these neurons are not necessary to express hedonically negative responses induced by bitter tastants (Fu et al., 2019). However, they did not explore their sufficiency. Our results showed that water deprivation temporarily gated LHA^{Vgat+} neurons to promote

quinine intake, and further demonstrated that their activation is sufficient to increase acceptance of an aversive tastant during water deprivation.

Furthermore, since LHA contains neurons responsive to aversive tastants (Li et al., 2013; Norgren, 1970; Schwartzbaum, 1988a) and noxious stimuli (Ono et al., 1986), we speculate about the possibility that a subset of LHA^{Vgat+} neurons, especially those exhibiting an anti-correlated response with sucrose's palatability, might be responsive to aversive stimuli. However, we believe it more likely that non-GABA^{Vgat} neurons (see Figure 2—figure supplement 1; perhaps a subset of glutamatergic LHA$^{Vglut2+}$ neurons (Fu et al., 2019)) underlie the aversive behaviors evoked by electrical LHA stimulation. Future studies should evaluate the neural responses evoked by aversive and noxious stimuli upon both LHA^{Vgat+} and LHA$^{Vglut2+}$ neurons.

The LHA is composed of multiple heterogeneous and overlapping populations based on the expression of genetic markers for neuropeptides, receptors, and proteins involved in the synthesis and vesicular packaging of neurotransmitters (Bonnavion et al., 2016). Thus, the LHA^{Vgat+} population can be further subdivided into GABA neurons expressing either the neuropeptide galanin (Qualls-Creekmore et al., 2017) or neurotensin (Nts) (Kurt et al., 2019). From these subpopulations, only the LHA GABA-Nts neurons recapitulate some (but not all) of the behavioral effects reported here. Unlike LHA^{Vgat+} neurons, a previous study found that LHA GABA-Nts neurons do not increase chow intake. Instead, they promote the liquid intake of palatable tastants (water, NaCl, and sucrose). In sated mice, chemogenetic activation of GABA-Nts increased the intake of bitter quinine, albeit with lower magnitude, when it was the only liquid available to eat chow food, a marked contrast to our findings with broad LHA GABAergic neurons activation. Although, they did not explore quinine intake, in the absence of chow food or in water-deprived mice. However, they performed a two-bottle

test and found that GABA-Nts neurons increased water intake over quinine, suggesting that these neurons cannot develop a preference for bitter tastants, similar to what we found for the LHA^{Vgat+} population. Also, similar to our findings, activation of LHA GABA-Nts induced drinking, but it was further facilitated by the presence of sucrose (Kurt et al., 2019). Thus, it will be interesting to determine the role that LHA GABA-Nts neurons play in encoding and potentiating sucrose's palatability. It follows that the LHA contains nested functions encoded in each subpopulation (or cell-types) that are then recruited selectively to exert a more refined control over feeding and reward.

A caveat of this study is that we employed bacterial artificial chromosomes (BAC) transgenic strain mouse, VGAT-ChR2, that constitutively expressed ChR2 in GABAergic neurons expressing the gene for the VGAT (Zhao et al., 2011). In this model, we cannot rule out unintended activation of GABAergic terminals coming from distal regions (Thoeni et al., 2020) a condition that also occurs with classic electrical stimulation. However, this transgenic model affords important advantages such as, consistent distribution and expression of ChR2 (Zeng and Madisen, 2012) and heritable transgene expression patterns across experimental cohorts (Ting and Feng, 2013), which increased reproducibility across animals tested. More importantly, it is a more selective model to characterize GABAergic neurons (excluding the glutamatergic component) and their effects recapitulating classical effects observed with electrical LHA stimulation (Coons and Cruce, 1968; Delgado and Anand, 1953; Mendelson, 1967; Mogenson and Stevenson, 1967; Phillips and Mogenson, 1968).

In summary, here we found LHA^{Vgat+} neurons could be an important hub that links stimulus-proximity and palatability related information to potentiate the palatability of nearby energy-

rich foods containing sucrose. Thus, LHA GABA neurons could be a potential drug target to modulate the palatability of caloric foods that produce obesity.

Materials and Methods

Animal subjects

We used 36 VGAT-ChR2 mice from both sexes and 8-16 weeks old (Number ID 014548; Jackson Laboratory, Sacramento, CA, USA). 21 wildtype (WT) littermates were used as a control, from both sexes. Mice were individually housed in laboratory home cages and maintained at temperature-controlled (22 ± 1° C) room with 12:12 h light-dark cycle, and unless otherwise mentioned, chow food (PicoLab Rodent Diet 20, MO, USA) and water was available *ad libitum*. For experiments with water restriction (Figures 1, 2, 7, and Figure 6—figure supplement 1), after behavioral testing, mice could drink water for 1 h daily. All procedures were performed with the approval of the CINVESTAV Animal Care and Use Committee. Experiments were conducted at the same time of the day from 11:00 AM to 2:00 PM.

Surgical procedures

For surgery, all mice were anesthetized with ketamine (100 mg/kg, i.p.) and xylazine (8 mg/kg, i.p.) and placed into a stereotaxic apparatus (Stoelting, IL, USA). Lidocaine (0.05 mL, subcutaneous) was applied as an analgesic, and ophthalmic ointment (hydrocortisone, neomycin, and polymyxin B) was used periodically to maintain eye lubrication. Antibiotic enrofloxacin (0.4 mL/kg) was injected for 3 days as a post-surgery treatment.

For experiments with opto-stimulation of LHA^{Vgat+} cell somas, a single multimode optic fiber 200 μm core diameter with a 0.39 NA (FT200UMT; Thorlabs, NJ, USA) was implanted

unilaterally targeting the LHA using the following coordinates: AP: -1.25 mm, ML: ± 1 mm, DV: -4.9 mm, from bregma. For electrophysiology recordings, a custom-made optrode was unilaterally implanted counterbalanced from both hemispheres (AP: -1.25 mm, ML: ± 1 mm, from bregma; DV: -5.2 mm ventral to dura). The optrode comprised of an array of 16 tungsten wires formvar coated (35 µm diameter) surrounding and protruding 1 mm the tip of a single multimode optic fiber. No significant differences were found between hemispheres, so data were pooled together (data not shown). To allowed recovery, all experiments began seven days after surgery.

Histology and Immunofluorescence

To verify optrode and optic fiber location, mice were sacrificed at the end of each experiment by an overdose of pentobarbital (150 mg/kg) and perfused with PBS, followed by 4% paraformaldehyde. Brains were fixed overnight in 4% paraformaldehyde and gradually replaced in different concentrations until reaching 30% sucrose concentration. For histology, brain slides (40 µm) were cut with a cryostat. Images were taken with a Nikon eclipse e200 and with progress gryphax microscope camera, using a 10x objective.

Free-floating brain slides (40 µm) were blocked with 1% BSA, 0.2% Triton in PBS for 30 min. Then, were washed with 0.2% Triton in PBS three times every 10 minutes, followed by the incubation with the primary antibodies: mouse anti-GAD 67 primary antibody (Millipore, Mab5406, 1:1000 dilution) and rabbit anti-GFP primary antibody (Invitrogen, A11122, 1:1000 dilution). Incubation overnight at 4°C. The next day, brain slides were washed with 0.2% Triton in PBS three times every 10 min. Then, were incubated with secondary antibodies: Alexa 647 goat anti-mouse (Invitrogen, A21235, 1:500 dilution) and Alexa 488 donkey anti-rabbit (Invitrogen, A21206, 1:500 dilution) by 90 min at room temperature. Then, we collocated DAPI to stain the nuclei. Brain slides were put on slides with a mounting medium

for fluorescence (Vectashield), and images were taken with a Leica confocal microscope using 63x objective.

Gustatory stimulus

Sucrose reagent-grade chemical quality (Sigma-Aldrich, Mexico City, Mexico) was used in the following concentrations: no sucrose, 3, 10, and 18 wt%. Quinine hydrochloride dihydrate (QHCl) reagent-grade was used at 0.004 wt% quinine (Sigma-Aldrich, Mexico City, Mexico). Artificial Saliva contained (mM): 4 NaCl, 10 KCl, 6 $NaHCO_3$, 6 $KHCO_3$, 0.5 $CaCl_2$, 0.5 $MgCl_2$, 0.24 K_2HPO_4, 0.24 KH_2PO_4 (Zocchi et al., 2017). We added 0.05 mM HCl to adjust to pH 7. The solutions were dissolved in distilled water and were maintained under refrigeration and used at room temperature. We also used 20 mg chocolate pellets (Bio-Serv, NJ, USA), chow food (PicoLab Rodent Diet 20, MO, USA), a high-fat diet with 45% kcal% fat (Research Diets, NJ, USA), granulated sugar cube, and cork.

Optogenetic stimulation

The intensity of a 473 nm laser was modulated by a DPSS system (OEM laser, UT, USA). Laser pulses were synchronized with behavioral experiments through Med Associates Inc. software and TTL signal generator (Med Associates Inc., VT, USA). The laser power at the tip of the fiber optic was measured with a fiber optic power meter (PM20A, Thorlabs, NJ, USA). A fixed power of 15 mW was used to produce a predicted irradiance of 109 mW/mm^2. For Figure 3, and Figure 1—figure supplement 1, the laser was turned “on” at different frequencies 2.5, 5, 10, 20, and 50 Hz semi-randomly, that is after all frequencies were tested, they will repeat randomly. For the other experiments, the laser was fixed at 50 Hz. The laser was 2 s on and 4 s off, with 10 ms pulse width and a duty cycle of 50%.

Behavioral Assays

Pre-stimulation task

Mice were placed in an operant conditioning chamber with a central port, but a door blocked the access to the sipper during the first 15 min. In this pre-stimulation period, each mouse was opto-stimulated with all pre-stimulation parameters following a Latin square design (described in the table below). Then, the door was opened, and a 10% sucrose solution was available during the next 15 min. During pre-stimulation period the laser was turned on for 2 s and 4 s off.

Pre-stimulation protocol schemes

Laser on	Sucrose access
0 min	15 min
5 min	15 min
10 min	15 min
15 min	15 min

Open loop stimulation task

Mice were opto-stimulated by alternating 5 min off and 5 min on blocks throughout the session (Nieh et al., 2016). During opto-stimulated blocks, the laser was turned “on” regardless of mice's behavior and spatial position in the chamber. The front panel of an operant conditioning chamber (Med Associates Inc, VT, USA) was equipped with one or three ports, each with a sipper where individual licks were registered by a contact lickometer (Med Associates Inc, VT, USA). For Figure 3, each session was presented with a different frequency (0, 2.5, 5, 10, 20, and 50 Hz), and mice had free access to a sucrose 10% solution in the central port. Whereas for Figures 4 and 5, mice had free access to water (central

sipper), a 3% sucrose solution (left sipper), and 18% sucrose solution (right sipper). Laterals sippers were counterbalanced across animals. This task was composed of 4 baseline days (without opto-stimulation, data not shown) and 11 test days (Figures 4 and 5).

For the open loop stimulation sessions, we video tracked the mouse's distance and head angle relative to each of the tree sippers, one containing sucrose 3%, water, or sucrose 18% (Figure 4— figure supplement 1). The sippers' position and three anatomical animal's points (nose, neck, and the base of the tail) were extracted using DeepLabCut Python package (Mathis et al., 2018; Nath et al., 2019). We define the mouse position as the coordinates (x and y) for the nose, whereas the head direction was a 2D vector going from the neck to the nose. For each video frame, the relative distance to each sipper was calculated (in pixels), and the relative angle between the head direction and position of each sipper (in degrees). An angle of 0º means the mouse is looking at the sipper, and 180º it is facing in the opposite direction. For distance measuring, 100 pixels correspond to approximately 6 cm. The mouse position and direction were extracted from the first laser pulse of the train of stimulation, and the following 6 s window was analyzed to find out if the mice initiated a licking behavior, at any of the 3 sippers. We then built a two-dimensional array containing the probability of licking any sipper given the mouse's distance and angle of the mouse during each first laser of each opto-stimulation train.

Closed-loop stimulation task

During 11 sessions, animals were tested in an operant conditioning chamber maintained in the same conditions described above. Opto-self-stimulation was delivered when the subject made a head entry in the central port by 2 s with a time out of 4 s post-stimulation. For Figure

6, the stimulus in the central port was replaced across sessions following the protocols described below.

Closed-loop stimulation protocol

Stimuli in central port	Sessions tested
Water	Last 5 sessions in Figure 5
Extinction (No opto-stimulation)	4
Water	3
Empty sipper	3
Water	3
0.004% Quinine	4
Airpuff	4
Unavoidable airpuff	3
Sucrose 18% (Water was placed in the sucrose 18% port)	4

Closed-loop stimulation task (one single bottle test)

Mice were put in a custom-made box of internal dimensions (18 x 13 x 7.5 cm), which front wall was equipped with one sipper (a contact lickometer with V-shape registered individual licks). 0.004% quinine or 18% sucrose were tested with sated and water-deprived mice during 3 and 2 sessions, respectively. Opto-self-stimulation (2 s on with a time out of 4 s) was delivered when mice made a head entry in the central port. Water-deprived mice had access to *ad libitum* water for 1 h after the session finished.

Open loop stimulation in an open field

Animals were placed in the center of a circular arena (50 cm of diameter). Three (Figure 4— figure supplement 2) or two (Figure 4— figure supplement 3) food plates were equidistant to each other, and each contained either Chow, high-fat diet, or granulated sugar cube. Mice

were opto-stimulated by alternating 5 min block with no-laser and 5 min laser block throughout the session. Laser was turned “on” regardless of mice's behavior and spatial position in the arena. All sessions were recorded and analyzed with bonsai software (https://open-ephys.org/bonsai). We calculated the mouse’ centroid at every frame and used that information to create a heatmap of its position. The distance of the mouse’s centroid relative to each stimulus was computed. An interaction occurred when the distance was below 60 mm, and the animal stayed there for at least 1 s. Food plates were weighted at the beginning and the end of each session.

Closed-loop in an open-field

Animals were placed in the center of a circular arena (50 cm of diameter). Four stimuli were located equidistant to each other, either wood cork, chow, chocolate pellets, or a sipper filled with 10% sucrose solution (Figure 5— figure supplement 2). During the session, a homemade computer vision program tracked in real-time the position of the subject. Each mouse needs to enter the designated area to receive opto-self-stimulation (2 s laser on and 4 s off). Mice need to leave and re-enter the designated area to begin a new trial.

Brief access test

To evaluate sucrose’s palatability, we used a brief access test in water-deprived mice. For this task, we used a licking spout consisting of independent stainless-steel needles (20-gauge) cemented together with dental acrylic at the tip of a sipper tube (Villavicencio et al., 2018). Each needle was connected to a solenoid valve (Parker, Ohio, USA) via a silicon tube. The volume of the drop (~2 μL) was calibrated before each session and maintained by using a pressurized control system. The sequence of a trial is as follows. At the beginning of the task, the sipper is extended in lick position. To start a new trial, the subject had to introduce its head into the central port to turned on the laser, then elicited a dry lick to start

the reward epoch (7s). During this period, a drop of a tastant was delivered every lick. Once the epoch was finished, the sipper was retracted during an inter-trial interval of 3 s, and then the sipper was re-extended into the central port. Tastant solutions (water, sucrose 3%, and sucrose 18%) were delivered in a semi-randomized order. The laser was turned on in a closed-loop protocol. Briefly, each head entry triggers the laser on for 2s (or 7s). The length of stimulation was modified between sessions for 2 s to 7s, in order to test whether licking could be evoked for a more extended period. At the end of the session, mice had access to *ad libitum* water for 1 h. Protocols are described below:

Brief access taste protocol

Laser on	Time on	# Sessions
All trials	2 s	6
Water trials	2 s	3
Sucrose 3% trials	2 s	3
Sucrose 18% trials	2 s	3
All trials	7 s	4
Water trials	7 s	3
Sucrose 3% trials	7 s	3
Sucrose 18% trials	7 s	3
Mock laser (sucrose 3% trials) *	7 s	3

*For mock laser, mice were connected to a false optic fiber, whereas the real laser was glued outside the skull to emit blue light.

In addition, in the same behavioral box, a brief access test was performed while the LH was recorded, followed by optogenetic tagging in the same session. Tastant solutions (artificial saliva, water, sucrose 3%, and 18 %) were delivered in a semi-randomized order.

We operationally defined sucrose's palatability as the enhancement of hedonically positive oromotor responses evoked by increasing sucrose concentrations (Berridge and Grill, 1983; Spector et al., 1998). For Figure 7, we analyzed palatability oromotor responses, using Peri-

Stimulus Time Histograms (PSTHs) aligned to the onset of opto-stimulation (Time = 0 s), whereas, Figure 1 neural responses were aligned to the first rewarded lick.

Electrophysiology

Neural activity was recorded using a Multichannel Acquisition Processor System (Plexon, Dallas TX, USA) interfaced with Med Associates to record behavioral events simultaneously (Gutierrez et al., 2010). Extracellular voltage signals were first amplified by an analog head-stage (Plexon, HST/16o25-GEN2-18P-2GP-G1), then amplified and sampled at 40 kHz. Raw signals were band-pass filtered from 154 Hz to 8.8 kHz and digitalized at 12 bits resolution. Only single neurons with action potentials with a signal to noise ratio of 3:1 were analyzed (Gutierrez et al., 2010). Action potentials were isolated online using a voltage-time threshold window and three principals' components contour templates algorithm. Furthermore, for all recordings, off-line spike sorting was performed (Plexon, offline sorter), and only single units with stable waveforms across the entire session were included in the analyses (Gutierrez et al., 2010) (see Figure 3—figure supplement 3).

Neuronal classification

Laser activated neurons ($pLHA^{Vgat}$; Figure 2) were detected by using two methods: 1) a Kruskal-Wallis to compare firing rates during a baseline (-1 to -0.04 s), against the activity during the presentation of laser (0 – 2 s, aligned to laser onset). 2) Cumsum statistic (Gutierrez et al., 2006) to obtain the first bin (1 ms resolution) after the first laser pulse that significantly increased the firing rate above baseline (from -20 to 0 ms). Only neurons showing a significant value in both tests were considered laser-activated $pLHA^{Vgat}$.

For Figure 1—figure supplement 1, the analysis was accomplished by using a Kruskal-Wallis test to compare firing rates during baseline (-1 to -0.04 s) period, against the activity during the presentation of laser (0 to 2 s) aligned to laser onset for all frequency tested. Neurons that significantly increased their firing rate during the laser stimulation were named "Activated," and neurons that decreased their activity were named "Inhibited" or non-LHA^{Vgat} neurons (Figure 2—figure supplement 1). Neurons with no significant modulation were classified as "unmodulated."

Optotagging stimulation protocol

To find the best parameter to opto-stimulate LHA^{Vgat+} neurons (Figure 1—figure supplement 1), mice were recorded in an optotagging task. In this task, the laser was presented at different frequencies (2.5, 5, 10, 20, and 50 Hz; Figure 1—figure supplement 1). LHA^{Vgat+} neurons were detected by a cumsum statistic described in Gutierrez et al., 2006. We used only 2.5 and 5 Hz frequency trials. Furthermore, to identify LHA^{Vgat+} neurons related to sucrose's palatability once the brief access test was finished (Figure 2), each mouse with an optrode was tested in the optotagging task laser was turned on 2 s at 50 Hz. ChR2-expressing cells LHA^{Vgat+} were those with an action potential evoked within ≤ 15 ms latency (Buonomano, 2003), as measured by a cumsum statistic mention above (Gutierrez et al., 2006).

Palatability-responsive neurons

To identify neurons whose firing rate correlated with palatability-induced oromotor responses, we used a best-window analysis following a previous study (Villavicencio et al., 2018). This method has been used to detect palatability-related activity in a brief access

test. Briefly, during each recording session, a palatability-index (PI) was calculated. The PI reflects the overall appetitive oromotor responses elicited by each tastant delivered in the session. It was computed by averaging the lick rate (number of licks/ 7s) during the entire reward epoch, including all the trials per session. In mice, the PI takes values between 0-8 Hz for sucrose stimuli (Glendinning et al., 2005). 0 Hz means animals ultimately rejected a solution in all trials, whereas 8 Hz indicates, they licked continuously during the entire reward epoch, thus reflecting a greater palatability response elicited by the tastant. Then, the firing rate of each neuron was calculated for a variety of time centers (from 0.25 to 6.75 s steps of 0.5 s) and in multiple window sizes (from 0.5 to 7 s in steps of 0.5 s), such that each window was estimated as the center ± (window size/2). We identified the windows where the mean firing rated was significantly different for at least one tastant delivered (i.e., tastants, using a Kruskal-Wallis test at an alpha of 0.05). Next, on a trial-by-trial basis, we computed Pearson's correlation coefficient (r; the alpha level at 0.05) between both the PI and the firing rate. The window with the largest absolute Pearson's correlation coefficient was selected as the "best-window." Thus, for the "best-window" and each statistical test (i.e., Kruskal-Wallis test and Pearson's correlation coefficient), a permutation assay was used for multiple-testing correction. This analysis was accomplished by shuffling the different tastant delivered 20,000 times (using the Matlab function "shuffle"). A corrected *p*-value was obtained using the following formula $p = (k+1)/(n+1)$, where k is the times in which a permuted distribution leads to a *p*-value smaller than the original *p*-value and n is the number of repetitions. Only time-windows with *p*'s < 0.05 in both tests (Kruskal-Wallis and Pearson Correlation) were considered as statically significant. Thus, the "best-window" is where the firing rate maximally correlated with the oromotor responses elicited by sucrose's palatability in a trial-by-trial basis. Results were qualitatively similar if we used the lick bout duration rather than the lick rate to compute the PI (data not shown) (Villavicencio et al., 2018).

Data Analysis

Data analysis was performed using MATLAB (The MathWorks Inc., Natick, MA) and GraphPad Prism (La Jolla, CA, USA). We used the mean ± sem and the α level at 0.05.

Competing interests: The authors declare that no competing interests exist.

Acknowledgments

This project was supported in part by Productos Medix 3247, Cátedra Marcos Moshinky, fundación Miguel Alemán Valdés, CONACyT Grants Fronteras de la Ciencia 63 and 10862, and Problemas Nacionales 464 (R.G.). Aketzali Garcia had a CONACyT doctoral fellowship, and data in this work is part of her doctoral dissertation in the Posgrado en Ciencias Biomédicas of the Universidad Nacional Autónoma de México. We want to thank Martin Vignovich and Professor Sidney A. Simon for helpful comments in an early version of this manuscript. We thank Mario Gil Moreno for building homemade optrode, and valuable help of Juan de Dios Rodriguez-Callejas during the acquisition of confocal microscope images. We also thank Ricardo Gaxiola, Victor Manuel García Gómez, and Fabiola Hernandez Olvera for invaluable animal care.

References

Anand BK, Brobeck JR. 1951. Localization of a “feeding center” in the hypothalamus of the rat. *Proceedings of the Society for Experimental Biology and Medicine Society for Experimental Biology and Medicine* **77**:323–4.

Berk ML, Finkelstein JA. 1982. Efferent connections of the lateral hypothalamic area of the rat: an autoradiographic investigation. *Brain Res Bull* **8**:511–526. doi:10.1016/0361-9230(82)90009-0

Berridge KC, Grill HJ. 1983. Alternating ingestive and aversive consummatory responses suggest a two-dimensional analysis of palatability in rats. *Behavioral neuroscience* **97**:563–73.

Berridge KC, Valenstein ES. 1991. What psychological process mediates feeding evoked by electrical stimulation of the lateral hypothalamus? *Behav Neurosci* **105**:3–14. doi:10.1037//0735-7044.105.1.3

Berthoud H-R, Münzberg H. 2011. The lateral hypothalamus as integrator of metabolic and environmental needs: from electrical self-stimulation to opto-genetics. *Physiol Behav* **104**:29–39. doi:10.1016/j.physbeh.2011.04.051

Bonnavion P, Mickelsen LE, Fujita A, de Lecea L, Jackson AC. 2016. Hubs and spokes of the lateral hypothalamus: cell types, circuits and behaviour. *J Physiol (Lond)* **594**:6443–6462. doi:10.1113/JP271946

Buonomano DV. 2003. Timing of neural responses in cortical organotypic slices. *Proc Natl Acad Sci USA* **100**:4897–4902. doi:10.1073/pnas.0736909100

Burnett CJ, Li C, Webber E, Tsaousidou E, Xue SY, Brüning JC, Krashes MJ. 2016. Hunger-Driven Motivational State Competition. *Neuron* **92**:187–201. doi:10.1016/j.neuron.2016.08.032

Chen Y, Lin Y-C, Zimmerman CA, Essner RA, Knight ZA. 2016. Hunger neurons drive feeding through a sustained, positive reinforcement signal. *Elife* **5**. doi:10.7554/eLife.18640

Coons EE, Cruce JA. 1968. Lateral hypothalamus: food current intensity in maintaining self-stimulation of hunger. *Science* **159**:1117–9. doi:10.1126/science.159.3819.1117

Delgado JM, Anand BK. 1953. Increase of food intake induced by electrical stimulation of the lateral hypothalamus. *The American journal of physiology* **172**:162–8. doi:10.1152/ajplegacy.1952.172.1.162

DiFeliceantonio AG, Coppin G, Rigoux L, Edwin Thanarajah S, Dagher A, Tittgemeyer M, Small DM. 2018. Supra-Additive Effects of Combining Fat and Carbohydrate on Food Reward. *Cell Metab* **28**:33-44.e3. doi:10.1016/j.cmet.2018.05.018

Ferssiwi A, Cardo B, Velley L. 1987. Gustatory preference-aversion thresholds are increased by ibotenic acid lesion of the lateral hypothalamus in the rat. *Brain Res* **437**:142–150. doi:10.1016/0006-8993(87)91535-6

Fu O, Iwai Y, Narukawa M, Ishikawa AW, Ishii KK, Murata K, Yoshimura Y, Touhara K, Misaka T, Minokoshi Y, Nakajima K. 2019. Hypothalamic neuronal circuits regulating hunger-induced taste modification. *Nat Commun* **10**:1–14. doi:10.1038/s41467-019-12478-x

Gigante ED, Benaliouad F, Zamora-Olivencia V, Wise RA. 2016. Optogenetic Activation of a Lateral Hypothalamic-Ventral Tegmental Drive-Reward Pathway. *PLoS ONE* **11**:e0158885. doi:10.1371/journal.pone.0158885

Glendinning JI, Chyou S, Lin I, Onishi M, Patel P, Zheng KH. 2005. Initial licking responses of mice to sweeteners: effects of tas1r3 polymorphisms. *Chem Senses* **30**:601–614. doi:10.1093/chemse/bji054

Grill, Berridge KC. 1985. Taste reactivity as a measure of the neural control of palatability.In Progress in Psychobiology and Physiological Psychology. Orlando, FL.: Academic Press. pp. 1–54.

Gutierrez R, Carmena JM, Nicolelis MAL, Simon SA. 2006. Orbitofrontal ensemble activity monitors licking and distinguishes among natural rewards. *J Neurophysiol* **95**:119–133. doi:10.1152/jn.00467.2005

Gutierrez R, Fonseca E, Simon SA. 2020. The neuroscience of sugars in taste, gut-reward, feeding circuits, and obesity. *Cell Mol Life Sci*. doi:10.1007/s00018-020-03458-2

Gutierrez R, Simon SA, Nicolelis MA. 2010. Licking-induced synchrony in the taste-reward circuit improves cue discrimination during learning. *The Journal of neuroscience : the official journal of the Society for Neuroscience* **30**:287–303. doi:10.1523/JNEUROSCI.0855-09.2010

Hoebel BG, Teitelbaum P. 1962. Hypothalamic control of feeding and self-stimulation. *Science* **135**:375–7.

Jennings JH, Rizzi G, Stamatakis AM, Ung RL, Stuber GD. 2013. The inhibitory circuit architecture of the lateral hypothalamus orchestrates feeding. *Science* **341**:1517–1521. doi:10.1126/science.1241812

Jennings JH, Ung RL, Resendez SL, Stamatakis AM, Taylor JG, Huang J, Veleta K, Kantak PA, Aita M, Shilling-Scrivo K, Ramakrishnan C, Deisseroth K, Otte S, Stuber GD. 2015. Visualizing hypothalamic network dynamics for appetitive and consummatory behaviors. *Cell* **160**:516–27. doi:10.1016/j.cell.2014.12.026

Karádi Z, Oomura Y, Nishino H, Scott TR, Lénárd L, Aou S. 1992. Responses of lateral hypothalamic glucose-sensitive and glucose-insensitive neurons to chemical stimuli in behaving rhesus monkeys. *J Neurophysiol* **67**:389–400. doi:10.1152/jn.1992.67.2.389

Kurt G, Woodworth HL, Fowler S, Bugescu R, Leinninger GM. 2019. Activation of lateral hypothalamic area neurotensin-expressing neurons promotes drinking. *Neuropharmacology* **154**:13–21. doi:10.1016/j.neuropharm.2018.09.038

Li JX, Yoshida T, Monk KJ, Katz DB. 2013. Lateral hypothalamus contains two types of palatability-related taste responses with distinct dynamics. *The Journal of neuroscience : the official journal of the Society for Neuroscience* **33**:9462–73. doi:10.1523/JNEUROSCI.3935-12.2013

Margules DL, Olds J. 1962. Identical “feeding” and “rewarding” systems in the lateral hypothalamus of rats. *Science* **135**:374–5. doi:10.1126/science.135.3501.374

Marino RAM, McDevitt RA, Gantz SC, Shen H, Pignatelli M, Xin W, Wise RA, Bonci A. 2020. Control of food approach and eating by a GABAergic projection from lateral hypothalamus to dorsal pons. *Proc Natl Acad Sci USA*. doi:10.1073/pnas.1909340117

Mathis A, Mamidanna P, Cury KM, Abe T, Murthy VN, Mathis MW, Bethge M. 2018. DeepLabCut: markerless pose estimation of user-defined body parts with deep learning. *Nat Neurosci* **21**:1281–1289. doi:10.1038/s41593-018-0209-y

Mendelson J. 1967. Lateral hypothalamic stimulation in satiated rats: the rewarding effects of self-induced drinking. *Science* **157**:1077–1079. doi:10.1126/science.157.3792.1077

Mogenson GJ, Stevenson JA. 1967. Drinking induced by electrical stimulation of the lateral hypothalamus. *Experimental neurology* **17**:119–27. doi:10.1016/0014-4886(67)90139-2

Nath T, Mathis A, Chen AC, Patel A, Bethge M, Mathis MW. 2019. Using DeepLabCut for 3D markerless pose estimation across species and behaviors. *Nat Protoc* **14**:2152–2176. doi:10.1038/s41596-019-0176-0

Navarro M, Olney JJ, Burnham NW, Mazzone CM, Lowery-Gionta EG, Pleil KE, Kash TL, Thiele TE. 2016. Lateral Hypothalamus GABAergic Neurons Modulate Consummatory Behaviors Regardless of the Caloric Content or Biological Relevance of the Consumed Stimuli. *Neuropsychopharmacology : official publication of the American College of Neuropsychopharmacology* **41**:1505–12. doi:10.1038/npp.2015.304

Nieh EH, Matthews GA, Allsop SA, Presbrey KN, Leppla CA, Wichmann R, Neve R, Wildes CP, Tye KM. 2015. Decoding neural circuits that control compulsive sucrose seeking. *Cell* **160**:528–541. doi:10.1016/j.cell.2015.01.003

Nieh EH, Vander Weele CM, Matthews GA, Presbrey KN, Wichmann R, Leppla CA, Izadmehr EM, Tye KM. 2016. Inhibitory Input from the Lateral Hypothalamus to the Ventral Tegmental Area Disinhibits Dopamine Neurons and Promotes Behavioral Activation. *Neuron* **90**:1286–1298. doi:10.1016/j.neuron.2016.04.035

Norgren R. 1970. Gustatory responses in the hypothalamus. *Brain Res* **21**:63–77. doi:10.1016/0006-8993(70)90021-1

Olds J, Milner P. 1954. Positive reinforcement produced by electrical stimulation of septal area and other regions of rat brain. *J Comp Physiol Psychol* **47**:419–427. doi:10.1037/h0058775

Ono T, Nakamura K, Nishijo H, Fukuda M. 1986. Hypothalamic neuron involvement in integration of reward, aversion, and cue signals. *J Neurophysiol* **56**:63–79. doi:10.1152/jn.1986.56.1.63

Phillips AG, Mogenson GJ. 1968. Effects of taste on self-stimulation and induced drinking. *J Comp Physiol Psychol* **66**:654–660. doi:10.1037/h0026523

Poschel BPH. 1968. Do biological reinforcers act via the self-stimulation areas of the brain? *Physiology & Behavior* **3**:53–60. doi:10.1016/0031-9384(68)90031-0

Qualls-Creekmore E, Yu S, Francois M, Hoang J, Huesing C, Bruce-Keller A, Burk D, Berthoud H-R, Morrison CD, Münzberg H. 2017. Galanin-Expressing GABA Neurons in the Lateral Hypothalamus Modulate Food Reward and Noncompulsive Locomotion. *J Neurosci* **37**:6053–6065. doi:10.1523/JNEUROSCI.0155-17.2017

Rolls ET. 2015. Taste, olfactory, and food reward value processing in the brain. *Prog Neurobiol* **127–128**:64–90. doi:10.1016/j.pneurobio.2015.03.002

Schwartzbaum JS. 1988a. Electrophysiology of taste, feeding and reward in lateral hypothalamus of rabbit. *Physiol Behav* **44**:507–526. doi:10.1016/0031-9384(88)90313-7

Schwartzbaum JS. 1988b. Electrophysiology of taste, feeding and reward in lateral hypothalamus of rabbit. *Physiol Behav* **44**:507–526. doi:10.1016/0031-9384(88)90313-7

Sclafani A. 1991. The Hedonics of Sugar and Starch.In R. C. Bolles (Ed.), The Hedonics of Taste. New York, NY.: Lawrence Erlbaum Associates, Inc. pp. 59–87.

Sharpe MJ, Marchant NJ, Whitaker LR, Richie CT, Zhang YJ, Campbell EJ, Koivula PP, Necarsulmer JC, Mejias-Aponte C, Morales M, Pickel J, Smith JC, Niv Y, Shaham Y, Harvey BK, Schoenbaum G. 2017. Lateral Hypothalamic GABAergic Neurons Encode Reward Predictions that Are Relayed to the Ventral Tegmental Area to Regulate Learning. *Current Biology* **27**:2089-2100.e5. doi:10.1016/j.cub.2017.06.024

Simerly RB. 2004. Anatomical Substrates of Hypothalamic Integration. In: The Rat Nervous System, The Rat Nervous System. Academic Press.

Spector AC, Klumpp PA, Kaplan JM. 1998. Analytical issues in the evaluation of food deprivation and sucrose concentration effects on the microstructure of licking behavior in the rat. *Behavioral neuroscience* **112**:678–94.

Stuber GD, Wise RA. 2016. Lateral hypothalamic circuits for feeding and reward. *Nature neuroscience* **19**:198–205. doi:10.1038/nn.4220

Teitelbaum P, Epstein AN. 1962. The lateral hypothalamic syndrome: recovery of feeding and drinking after lateral hypothalamic lesions. *Psychological review* **69**:74–90.

Ter Horst GJ, Luiten PG. 1987. Phaseolus vulgaris leuco-agglutinin tracing of intrahypothalamic connections of the lateral, ventromedial, dorsomedial and paraventricular hypothalamic nuclei in the rat. *Brain Res Bull* **18**:191–203. doi:10.1016/0361-9230(87)90190-0

Thoeni S, Loureiro M, O'Connor EC, Lüscher C. 2020. Depression of Accumbal to Lateral Hypothalamic Synapses Gates Overeating. *Neuron*. doi:10.1016/j.neuron.2020.03.029

Ting JT, Feng G. 2013. Development of transgenic animals for optogenetic manipulation of mammalian nervous system function: progress and prospects for behavioral neuroscience. *Behav Brain Res* **255**:3–18. doi:10.1016/j.bbr.2013.02.037

Urstadt KR, Berridge KC. 2020. Optogenetic mapping of feeding and self-stimulation within the lateral hypothalamus of the rat. *PLoS ONE* **15**:e0224301. doi:10.1371/journal.pone.0224301

Valenstein ES, Cox VC. 1970. Influence of hunger, thirst, and previous experience in the test chamber on stimulus-bound eating and drinking. *J Comp Physiol Psychol* **70**:189–199. doi:10.1037/h0028708

Valenstein ES, Cox VC, Kakolewski JW. 1968. Modification of Motivated Behavior Elicited by Electrical Stimulation of the Hypothalamus. *Science* **159**:1119–1121. doi:10.1126/science.159.3819.1119

Valenstein ES, Phillips AG. 1970. Stimulus-bound eating and deprivation from prior contact with food pellets. *Physiology & Behavior* **5**:279–282. doi:10.1016/0031-9384(70)90099-5

Villavicencio M, Moreno MG, Simon SA, Gutierrez R. 2018. Encoding of Sucrose's Palatability in the Nucleus Accumbens Shell and Its Modulation by Exteroceptive Auditory Cues. *Front Neurosci* **12**:265. doi:10.3389/fnins.2018.00265

Yamamoto T, Matsuo R, Kiyomitsu Y, Kitamura R. 1989. Response properties of lateral hypothalamic neurons during ingestive behavior with special reference to licking of various taste solutions. *Brain Res* **481**:286–297. doi:10.1016/0006-8993(89)90805-6

Zeng H, Madisen L. 2012. Mouse transgenic approaches in optogenetics. *Prog Brain Res* **196**:193–213. doi:10.1016/B978-0-444-59426-6.00010-0

Zhang X, van den Pol AN. 2017. Rapid binge-like eating and body weight gain driven by zona incerta GABA neuron activation. *Science* **356**:853–859. doi:10.1126/science.aam7100

Zhao S, Ting JT, Atallah HE, Qiu L, Tan J, Gloss B, Augustine GJ, Deisseroth K, Luo M, Graybiel AM, Feng G. 2011. Cell type-specific channelrhodopsin-2 transgenic mice for optogenetic dissection of neural circuitry function. *Nature methods* **8**:745–52.

Zocchi D, Wennemuth G, Oka Y. 2017. The cellular mechanism for water detection in the mammalian taste system. *Nat Neurosci* **20**:927–933. doi:10.1038/nn.4575

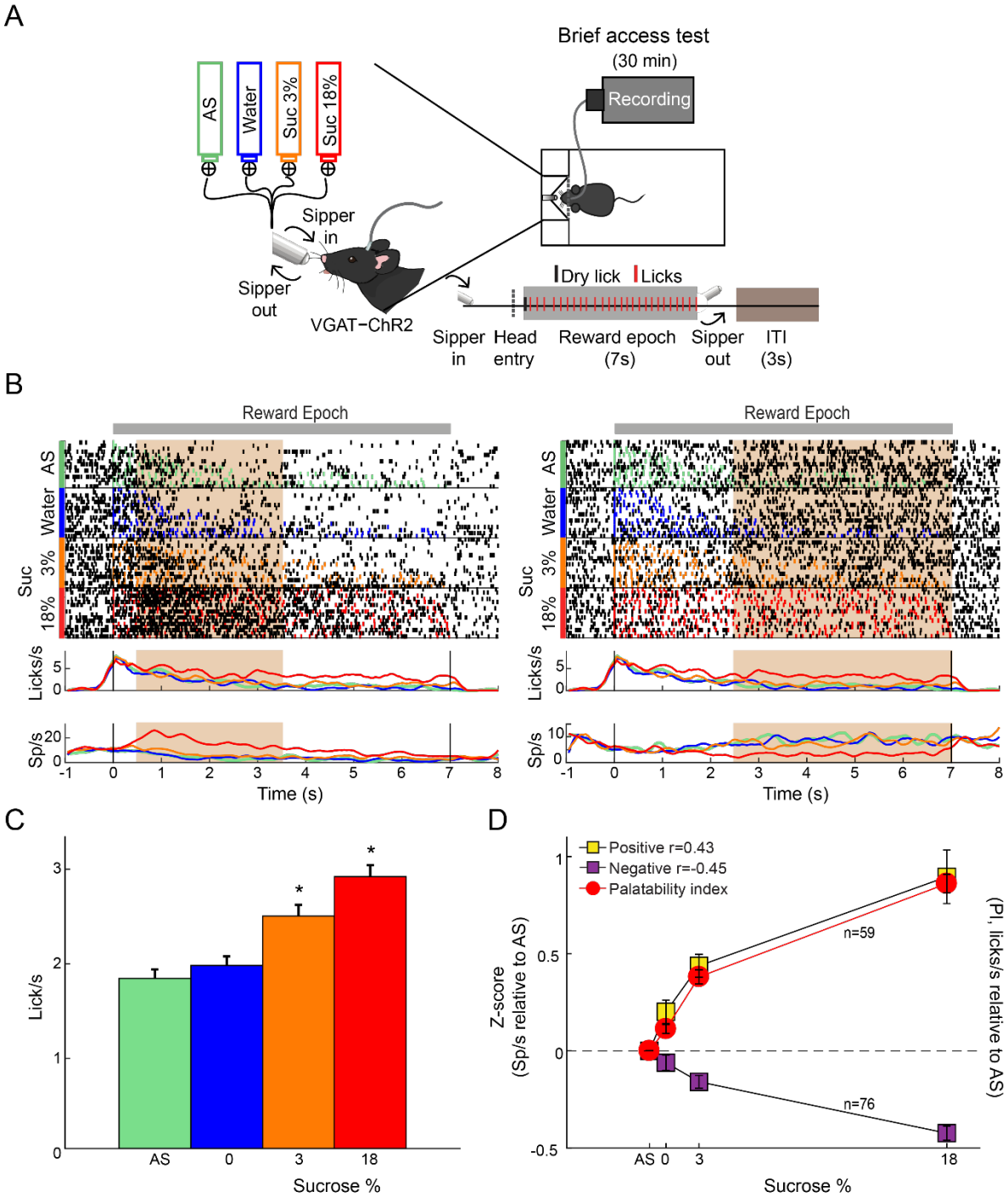
A
Brief access test
(30 min)
Recording
AS
Water
Suc 3%
Suc 18%
Sipper in
Sipper out
VGAT−ChR2
Dry lick
Licks
Sipper in
Head entry
Reward epoch (7s)
Sipper out
ITI (3s)
B
Reward Epoch
Reward Epoch
AS
Water
Suc 3%
18%
Licks/s
Sp/s
Time (s)
C
Lick/s
AS
0
3
18
Sucrose %
D
Positive r=0.43
Negative r=-0.45
Palatability index
Z-score (Sp/s relative to AS)
(PI, licks/s relative to AS)
n=59
n=76
Sucrose %

Figure 1. LHA neurons process palatability-related information. (**A**) Brief access taste and optotagging setup depicting a behavioral box equipped with a computer-controlled retractile sipper that for each lick independently delivers a drop of artificial saliva (AS), water, sucrose 3%, or 18% concentrations. After a head entry (dashed line), the first dry lick (black line) enables the 7 s reward epoch. During this period, in each lick (red), a drop of the four tastants was randomly delivered. After the reward epoch, the sipper was retracted for an Intertrial Interval (ITI) of 3 s and then re-extended to start a new trial. (**B**) Representative raster plot of two LHA neurons recorded while mice performed a brief access test. Spikes are plotted as black ticks, whereas licks for each tastant are in color-coded (green, AS; blue, water; orange, sucrose 3%; red, sucrose 18%). Below are corresponding peristimulus time histograms (PSTHs) of lick rate (Licks /s) and firing rate (Spikes/s; Sp/s) as a function of trial type. Neuronal responses were aligned (Time = 0 s) to the first rewarded lick. The brown rectangles depict the "best" window with the maximum Pearson correlation coefficient between firing rates and sucrose's palatability index (PI). The left and right raster plots displayed two neurons with a positive and negative correlation, respectively. (**C**) Average lick rate during the entire reward epoch, reflecting greater palatability as a function of sucrose concentration. (**D**) Z-score normalized activity (relative to AS trials) for LHA neurons with either positive or negative correlation against PI (red circles).

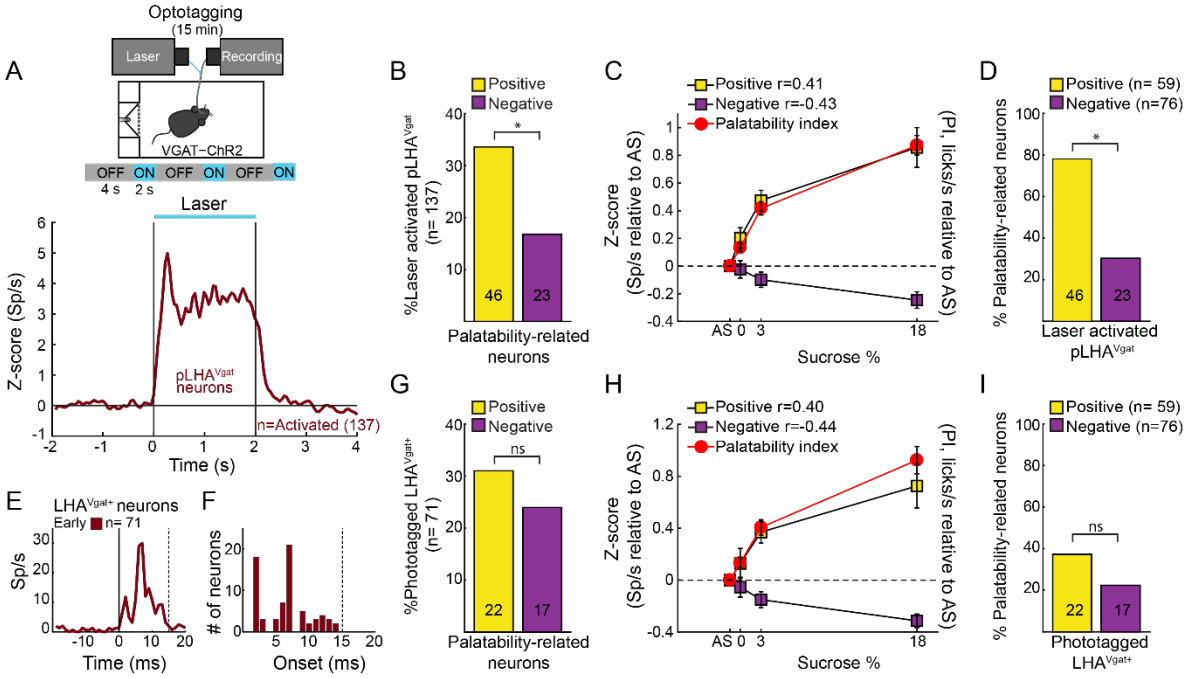

Figure 2. A subpopulation of LHA^{Vgat+} neurons encodes sucrose's palatability. (**A**) To confirm the LHA^{Vgat+} neurons' identity after the brief access test, we performed laser opto-stimulation in a cycle 2 s on (at 50 Hz, Figure 1—figure supplement 1) and 10 s off over 15 min session. In this phase, mice had no access to the sipper (*above panel*), *below* the normalized Z-score population activity of all 284 LHA neurons recorded from 3 VGAT-ChR2 mice. Responses were aligned to laser onset (Time = 0 s), relative to baseline (-1 to 0 s) activity, and red corresponds to activated putative pLHA^{Vgat} neurons. (**B**) Percentage of laser-activated pLHA^{Vgat+} neurons whose activity (in the brief access test) also correlated positively or negatively with the sucrose's PI. * $p < 0.01$, chi-square. (**C**) Z-score activity (relative to AS) for all activated pLHA^{Vgat} neurons and its correlation with the sucrose's PI. (**D**)

Percentage of Positive or Negative laser-activated palatability-related neurons. * $p < 0.0001$, chi-square (**E**) PSTH of identify (opto-tagged) LHA^{Vgat+} neurons exhibiting early evoked responses (i.e., ChR2 expressing cells). (**F**) Histogram of opto-tagged LHA^{Vgat+} neurons with evoked early responses (latencies < 15 ms) from laser onset. (**G-I**) same conventions as in (**B-D**) but for opto-tagged LHA^{Vgat+} neurons encoding sucrose's palatability.

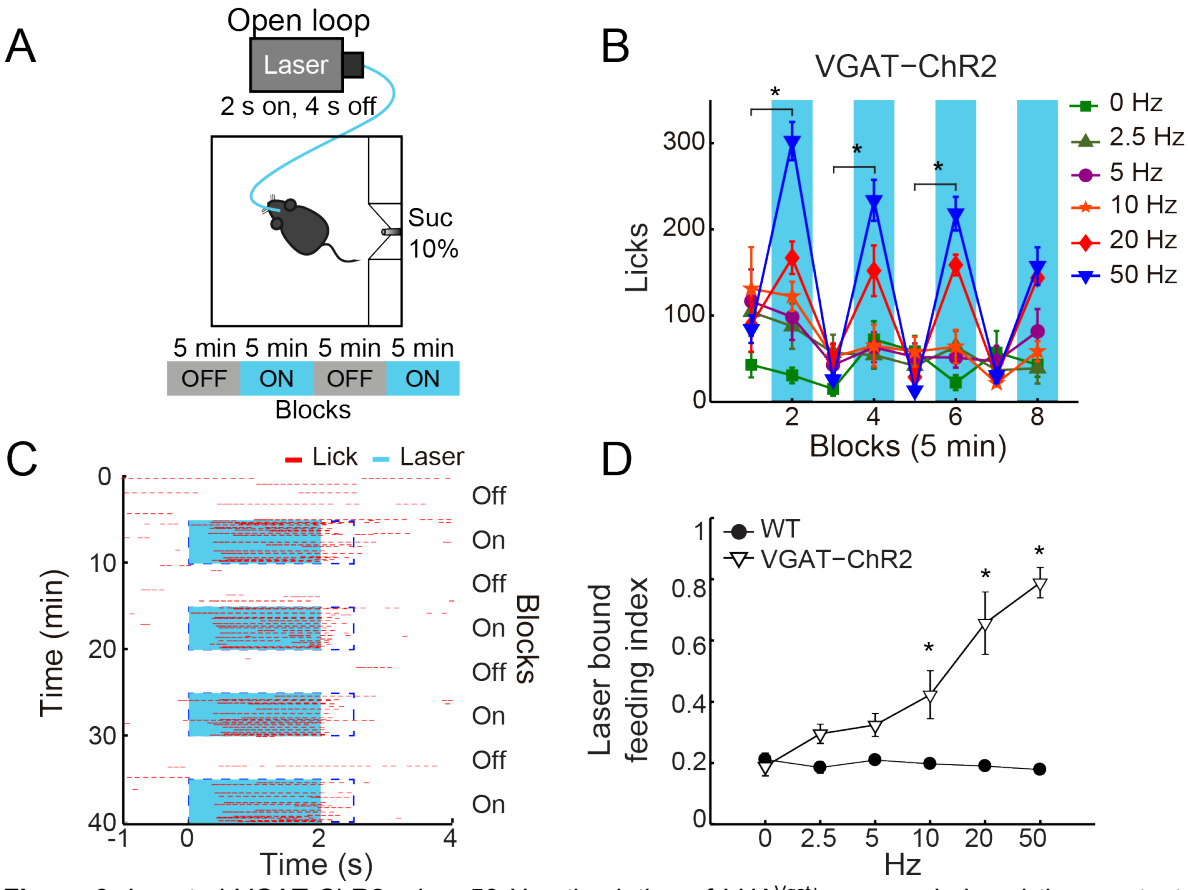

Figure 3. In sated VGAT-ChR2 mice, 50 Hz stimulation of LHA^{Vgat+} neurons induced the greatest intake of sucrose. (**A**) Behavioral setup for open-loop stimulation, where the laser was turned on regardless of the mice's behavior. The box was equipped with a central sipper where mice had free access to 10 % sucrose. Open-loop stimulation comprised 5 min block without laser followed by opto-stimulation for 5 min, in a cycle 2 s on – 4 s off, during a 40 min session. VGAT-ChR2 (n = 3) and WT (n = 5) mice received stimulation of only one of the following frequencies in ascending order per session 0, 2.5, 5, 10, 20, and 50 Hz. (**B**) Opto-stimulation of LHA^{Vgat+} neurons induced sucrose (10%) intake in a frequency-dependent manner that peaked at 50 Hz. * denote statistically significant difference ($p < 0.001$) between no-laser and laser stimulated blocks at 50 Hz. Besides mice were sated, the lower intake at 0 Hz could be due to the lack of experience drinking in the novel box. (**C**) Representative raster plot of open-loop stimulation from a VGAT-ChR2 mouse at 50 Hz. Lick responses (red ticks) were aligned to laser onset (blue rectangles, opto-stimulation period). The laser bound index was the number of licks within 2.5 s from laser onset (dashed blue rectangles) divided

by total licks. (**D**) The laser bound feeding index of VGAT-ChR2 increased as a function of the laser frequency. * $p < 0.01$ asterisks denote statistically significant difference relative to WT mice, using a Two-way ANOVA followed by the Holm Sidak test. In this and other figures, data represent mean ± SEM.

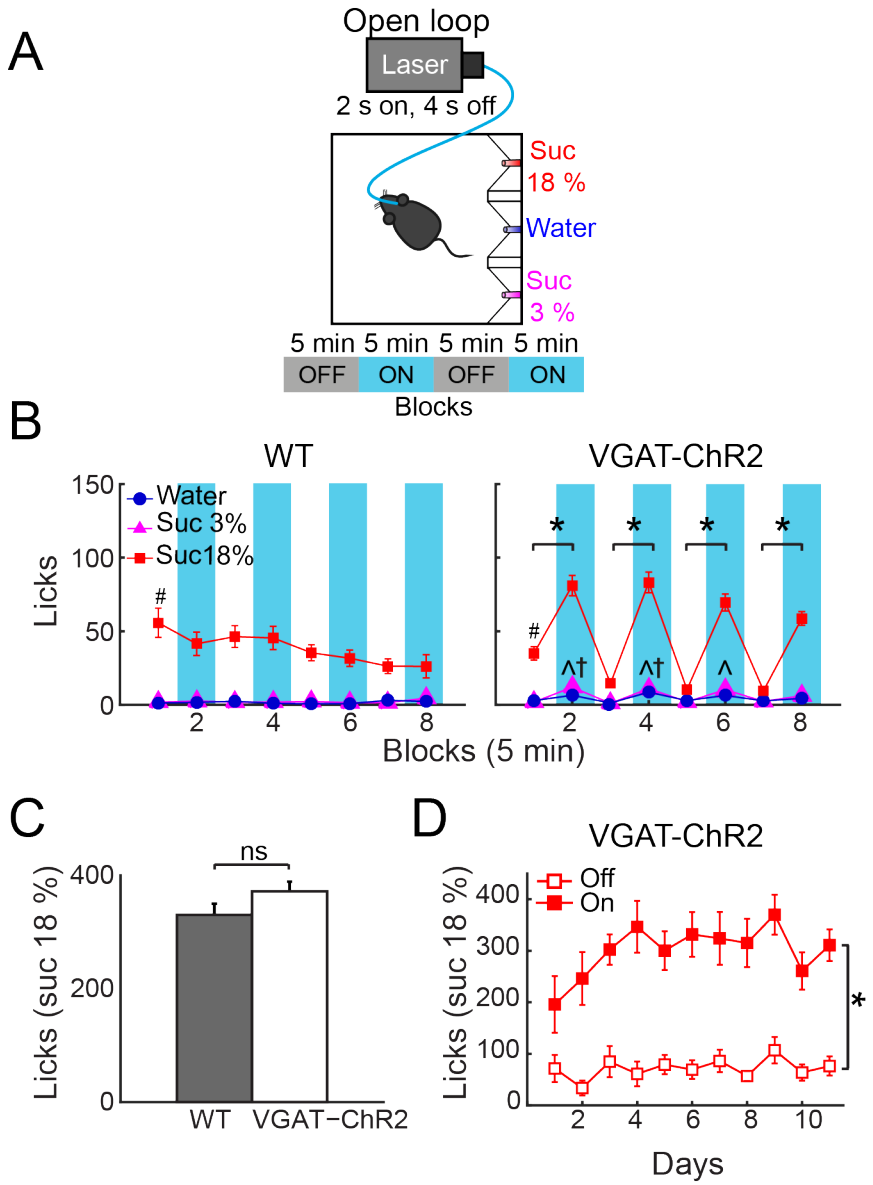

Figure 4. Open loop stimulation of LHA^{Vgat+} neurons biases consumption towards the most palatable tastant and reinforce intake during opto-stimulation. (**A**) Behavioral protocol. Sated mice (n = 6 WT and n = 12 VGAT-ChR2) were located in an operant box equipped with three ports. The left port contained sucrose 18%, the central port water, and the right port sucrose 3%, counterbalanced across

individuals. For details of open loop, see Figure 3A. (**B**) *Left and right panel*, number of licks for each gustatory stimulus for WT and VGAT-ChR2 mice. Note that the VGAT-ChR2 mice increased consumption of the most palatable stimuli available (sucrose 18%) mainly in opto-stimulated blocks (blue rectangles), while it decreased intake in blocks without laser. (**C**) Total licks gave to sucrose 18%. (**D**) Licks for sucrose 18% during blocks with or without laser across days. Data were expressed as mean ± SEM. * $p < 0.0001$. Asterisks indicate a significant difference between laser and no-laser blocks. # $p < 0.0001$ statistically significantly different between sucrose 18% and the other stimuli. ^ $p < 0.01$ between WT and VGAT-ChR2 for sucrose 3%. † $p < 0.01$ higher intake of water of VGAT-ChR2 compared with WT, using a two-way ANOVA and RM ANOVA followed by the Holm Sidak test.

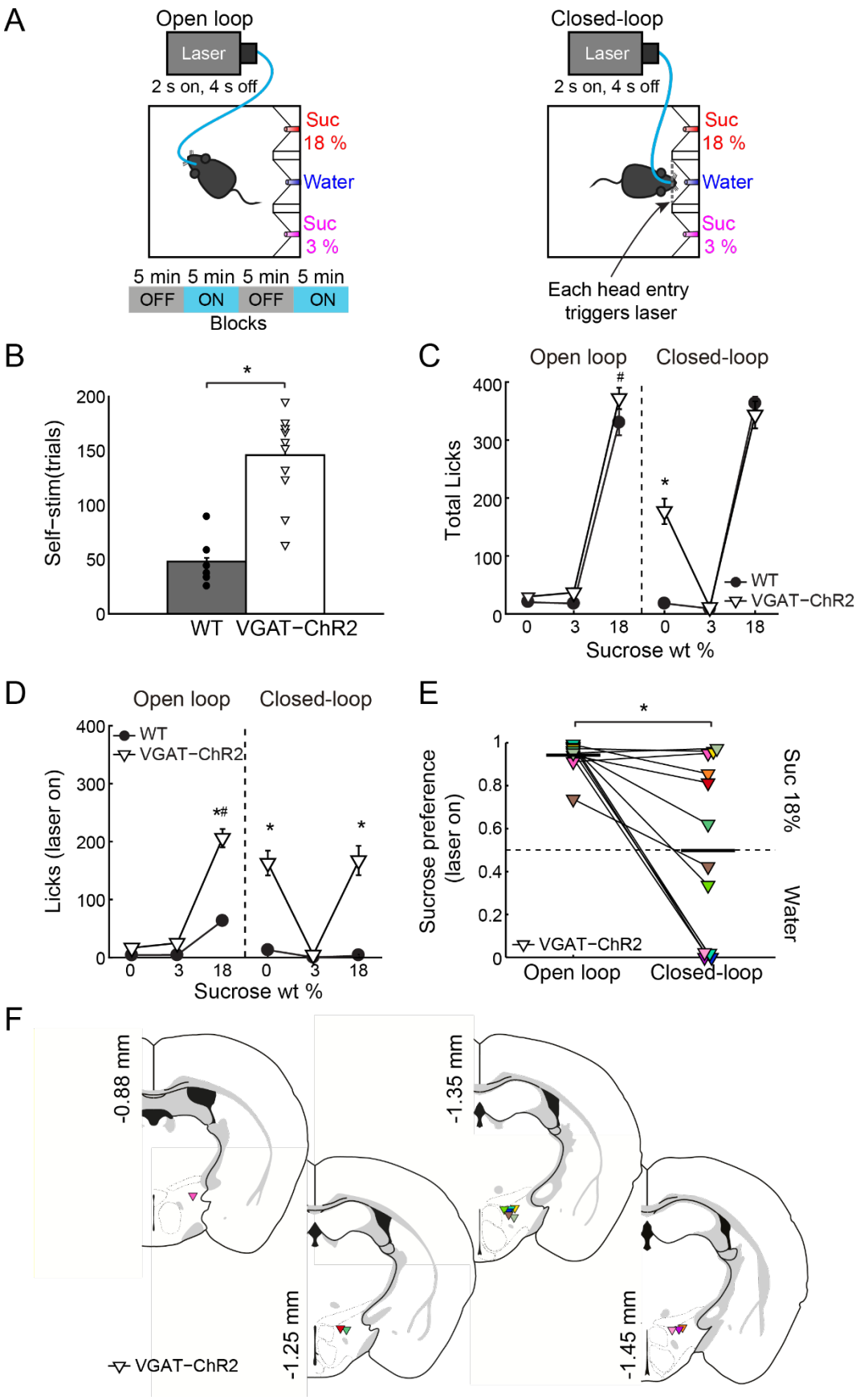
A
Open loop
Laser
2 s on, 4 s off
Suc
18 %
Water
Suc
3 %
5 min 5 min 5 min 5 min
OFF ON OFF ON
Blocks
Closed-loop
Laser
2 s on, 4 s off
Suc
18 %
Water
Suc
3 %
Each head entry
triggers laser
B
Self−stim(trials)
WT VGAT−ChR2
C
Open loop
Closed-loop
Total Licks
WT
VGAT−ChR2
Sucrose wt %
D
Open loop
Closed-loop
Licks (laser on)
WT
VGAT−ChR2
Sucrose wt %
E
Sucrose preference
(laser on)
Suc 18%
Water
VGAT−ChR2
Open loop
Closed-loop
F
-0.88 mm
-1.35 mm
-1.25 mm
-1.45 mm
VGAT−ChR2

Figure 5. If stimulation occurred near the less palatable stimulus, LHA^{Vgat+} neurons induced water intake despite sucrose. (**A**) For the open loop stimulation, the laser was activated (2s on, 4s off) regardless of behavior and mice position. Same mice and conventions as in Figure 4*A*. In the closed-loop configuration, the laser was triggered by a head entry in the central port. (**B**) Number of laser activations during closed-loop protocol. The VGAT-ChR2 mice self-stimulate more than the WT mice. Each dot and triangle represent a single mouse. (**C**) The total number of licks for each stimulus given during the entire session. In the open loop both mice groups licked more sucrose 18% than water or sucrose 3%. However, in the closed-loop configuration, the VGAT-ChR2 consumed more water (0 % sucrose) than the WT mice. (**D**) The number of licks evoked during 2.5 s after laser onset for each gustatory stimulus. (**E**) The water-sucrose 18% preference index from VGAT-ChR2 mice during photostimulation was defined as the number of licks of 18% sucrose divided by total licks for sucrose 18% + water. Thus, values higher than 0.5 indicate sucrose 18%, and values lower than 0.5 prefer water. Some VGAT-ChR2 mice preferred water over sucrose. The horizontal black lines indicate mean preference in both stimulation protocols. (**F**) Optic fiber location in the LHA of VGAT-ChR2 mice. * $p < 0.0001$ asterisks indicate significant differences compared with WT mice and stimulation protocols. # $p < 0.0001$ between sucrose 18% the other stimuli. Unpaired-Student t-test and two-way ANOVA followed by the Holm Sidak test.

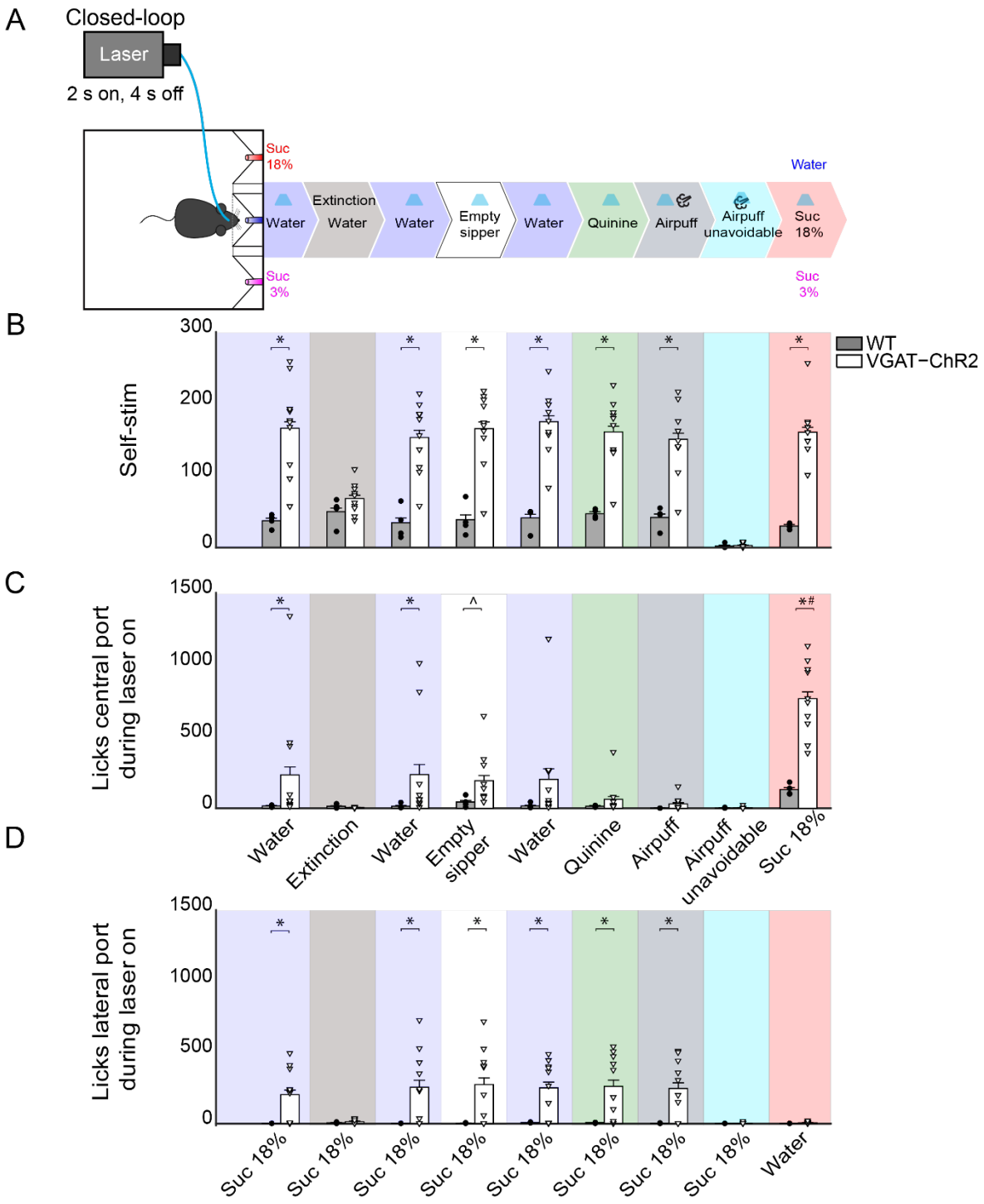

Figure 6. LHA^{Vgat+} neurons do not induce the intake of a bitter tastant, nor an unavoidable aversive stimulus, but it increases the consumption of sucrose. (**A**) Schematic of behavioral setup showing stimuli delivered at central port. The water stimulus in the central port was replaced by an empty sipper, quinine, or airpuff. In all phases, head-entry in the central port triggered the laser, except in the airpuff unavoidable condition, where the first lick delivered both the laser and the airpuff. Finally,

the airpuff in central port was replaced by sucrose 18%. (**B**) The number of opto-self-stimulations given for each stimulus. The VGAT-ChR2 mice performed more self-stimulations compared with WT, except during extinction sessions and when the airpuff was unavoidable. (**C**) The number of licks given to the central port. The licks in the central port decreased when an aversive stimulus was present, such as quinine or airpuffs. In contrast, a non-edibles stimulus such as an empty sipper elicited more licks from VGAT-ChR2 mice ($p < 0.05$). Moreover, when sucrose 18% was in the central port, VGAT-ChR2 group increased its consumption substantially compared with WT. (**D**) The number of licks in the lateral port containing sucrose 18% during opto-self-stimulation. The intake of the lateral port of sucrose 3 % is not shown because it was neglectable. Each dot and triangle represent a single individual. ^ Denote statistically significant differences ($p < 0.0001$) relative to WT. Unpaired-Student t-test. * $p < 0.05$ relative to WT group. # $p < 0.05$ between sucrose 18% relative to other stimuli delivered at the central port. Two-way ANOVA followed by the Holm Sidak test.

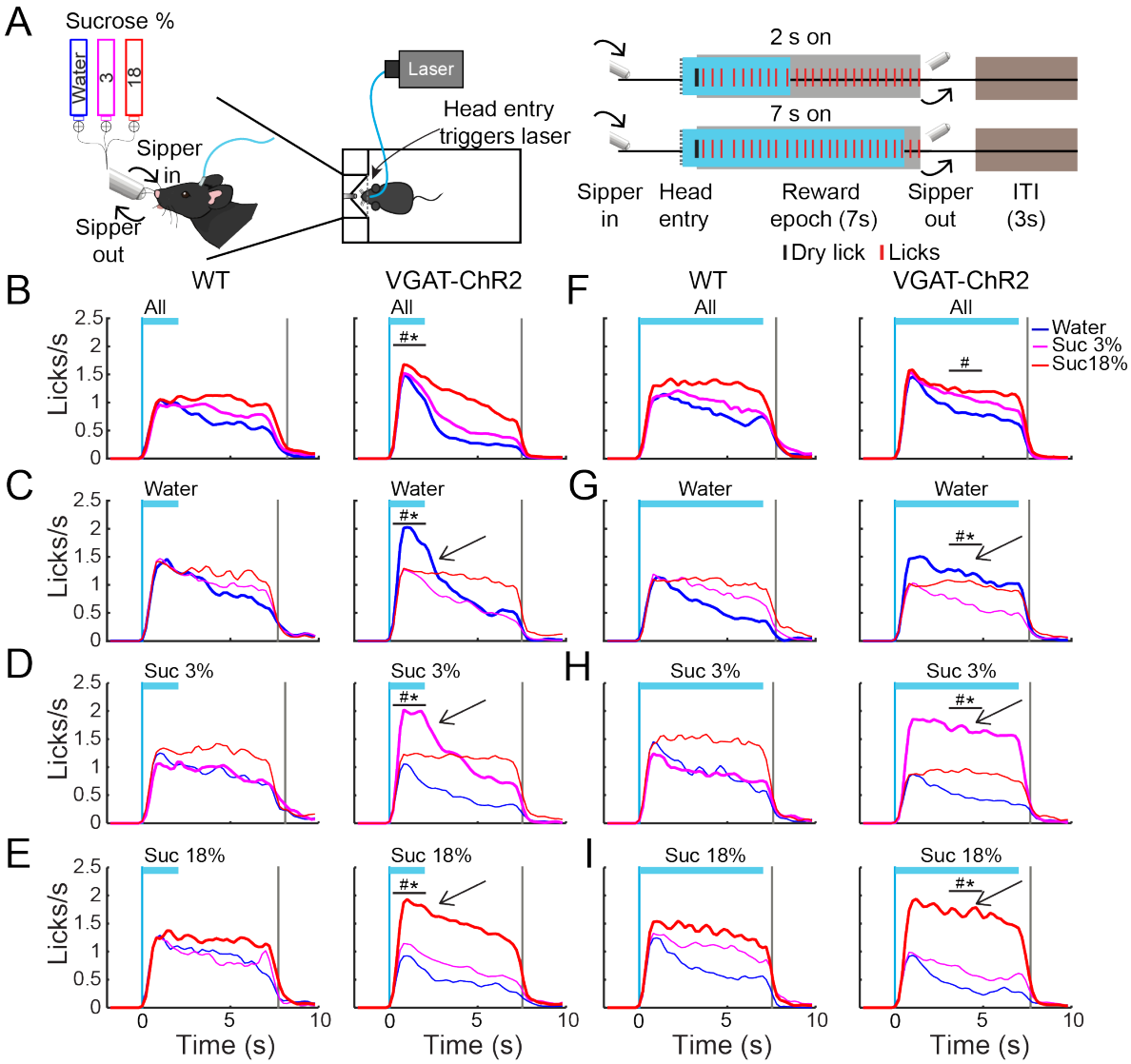

Figure 7. Activation of LHA GABA neurons enhances water and sucrose's palatability. (**A**) Closed-loop stimulation during the brief access test. *Left panel,* behavioral setup. The box contained a sipper that delivered a ~2 µL drop of either water, sucrose 3%, or 18% per lick. *Right panel*, schematics of

the structure of a trial. A head entry in the port (dashed vertical line) triggered opto-self-stimulation, at 50 Hz, in some sessions for 2 s and others for 7 s (blue rectangles). The reward epoch begins with the first dry lick on the sipper (black tick) and always last 7s (gray rectangles). During the reward epoch, a drop of tastant was delivered in each lick (red marks). At the end of it, the sipper was retracted, and an Inter Trial Interval (ITS) of 3 s began. (**B-E**) Data of closed-loop for 2s stimulation in the Reward epoch. PSTH of lick rate of WT (left panel) and VGAT-ChR2 mice (*right panel*) aligned (Time = 0 s) to laser onset. Opto-self-stimulation was delivered during all trials (B) or during only water trials (C, see arrow), or sucrose 3% (D), or 18 % (E). (**F-I**) Licking responses but during 7 s opto-self-stimulation. Same conventions as in B-E. The vertical blue line indicates laser onset and gray line the end of the reward epoch. The horizontal blue line indicates opto-self-stimulation window. * Indicates a significant difference ($p < 0.05$) relative to WT group. # significant differences ($p < 0.05$) among stimuli.

Supplementary Figures

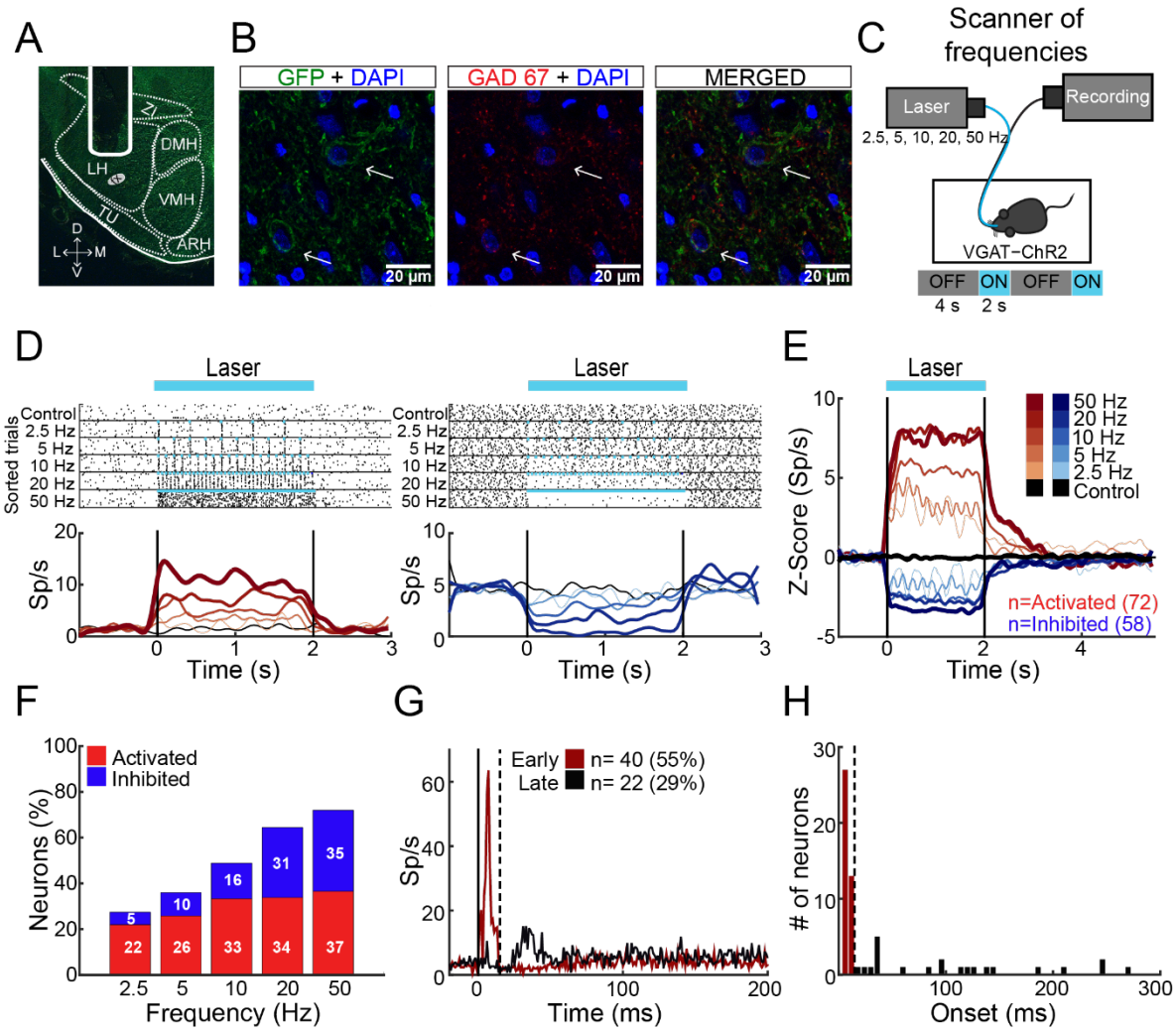

Figure 1— figure supplement 1. The 50 Hz stimulation evoked the largest LHA neuronal responses. (**A**) Representative location of an optrode in LHA of VGAT-ChR2 mice. (**B**) Confocal images from LHA immunostained for GFP (green), GAD67 (red), and DAPI (blue). Arrows indicate the colocalization of ChR2-EYFP and GAD67 (see merged). (**C**) Schematic of optrode recordings in LHA during control trials (with no-laser) and opto-stimulation at 2.5, 5, 10, 20, and 50 Hz delivered randomly. In each trial, the laser had a cycle of 2 s on and 4 s off. (**D**) Representative raster plots of two neurons recorded in LHA, the first one was activated (left panel), and the second inhibited (right panel) during opto-stimulation. Spiking responses were aligned (Time = 0 s) to the first laser pulse. Black ticks depict action potentials and blue marks laser pulses. For visualization purposes, it is only shown laser pulses in the first trial for each trial type. Below are the corresponding PSTHs (firing rates, Sp/s). Red and blue ascending gradients indicate the frequency of stimulation (see E for the color bar). Black trace represents activity during control trials without laser. Vertical black lines indicate laser onset (Time = 0 s) and offset (Time = 2 s), respectively. (**E**) Normalized Z-score population responses of LHA neurons recorded from n = 5 VGAT-ChR2 mice. Red and blue colors depict activated or inhibited responses, respectively, relative to baseline (-1 to 0 s), thickness, and gradient colors indicate higher stimulation frequencies. Black trace illustrates neural activity during control trials for all recorded neurons (n = 186). (**F**) Percentage of neurons recruited as a function of stimulation frequency. (**G**) From the subpopulation of laser-activated neurons, we computed the percentage of neurons with either Early (ChR2-expressing, red line) or Late evoked response (non-

expressing, black line) after the first pulse at 2.5 and 5 Hz, because, at these frequencies, the inter-pulse-interval allows to measure evoked action potentials within 200 ms without the interference of the second laser pulse. (**H**) Histogram of ChR2 expressing cells (Early; red) and Late responsive (black) neurons. In G and H, the dashed black lines indicate the 15 ms criteria to split Early from Late responses.

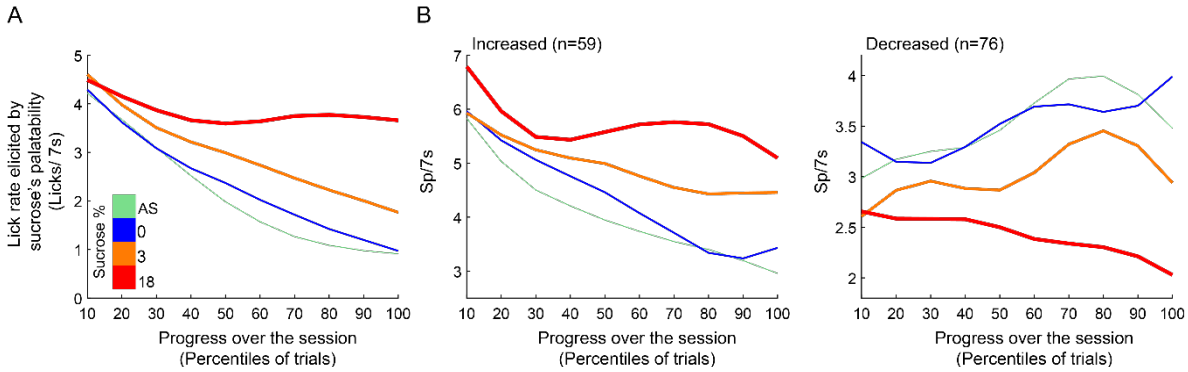

Figure 1— figure supplement 2. LHA palatability-related neurons dynamically track de changes in lick rate elicited by sucrose's palatability throughout the session. (**A**) Population PSTHs of the lick rates given in the Reward epoch (Licks/7s) as a function of trial type, divided into blocks of 10th percentiles of trials each. (**B**) Population PSTHs of the firing rate during the Reward epoch (spikes/ 7s) of the palatability-related neurons throughout the session for each trial type. *Left panel* depicts neurons that fired more to higher sucrose concentrations (positive sucrose's palatability correlation; Figure 1D yellow), whereas, *right panel* illustrates neurons with decreasing firing rates as the sucrose concentration increased (i.e., negative correlation with sucrose's palatability; Figure 1D purple).

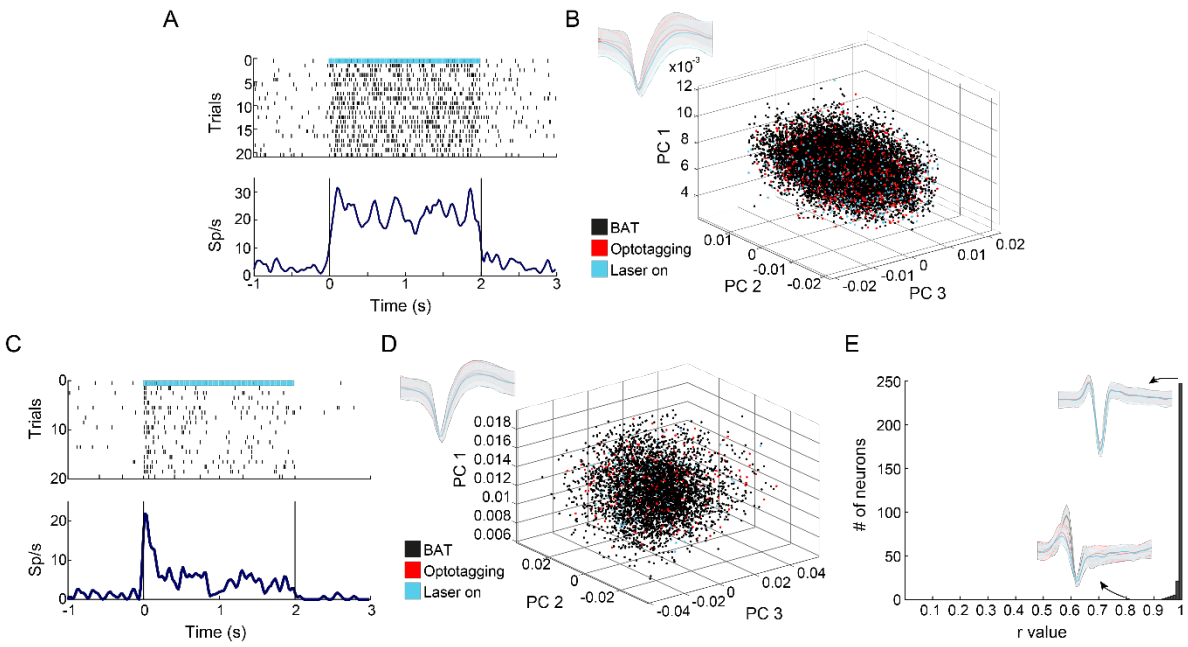

Figure 1— figure supplement 3. Waveform stability in extracellular recordings of LHA neurons across the brief-access test (BAT) and the optotagging session. (**A**) Representative raster plot of a LHA^{Vgat+} neurons recorded during the optotagging session. Spiking responses were aligned (Time = 0 s) to the first laser pulse. Black ticks depict action potentials and blue marks on top, laser pulses (at 50 Hz). For visualization purposes, it is only shown laser pulses in the first trial. Below, PSTHs (Spikes /s, Sp/s). Vertical black lines indicate laser onset (Time = 0 s) and offset (Time = 2 s), respectively. (**B**) Inset upper left depicts average waveforms of a single neuron showed in A across the BAT (black), the optotagging stimulation (red), and when the laser was turned "on" (blue). Right, each dot represents an action potential during the entire session (same color-coded). Values are plotted in a three-dimensional space computed with the first three principal components (PCs) of the waveforms. (**C-D**) Same conventions as in (**A-B**). (**E**) Histogram of the Pearson correlation coefficients of waveforms recorded during BAT against those recorded in the optotagging session. Waveforms depict two examples, one depicting the worst and the other the best correlation included in analysis.

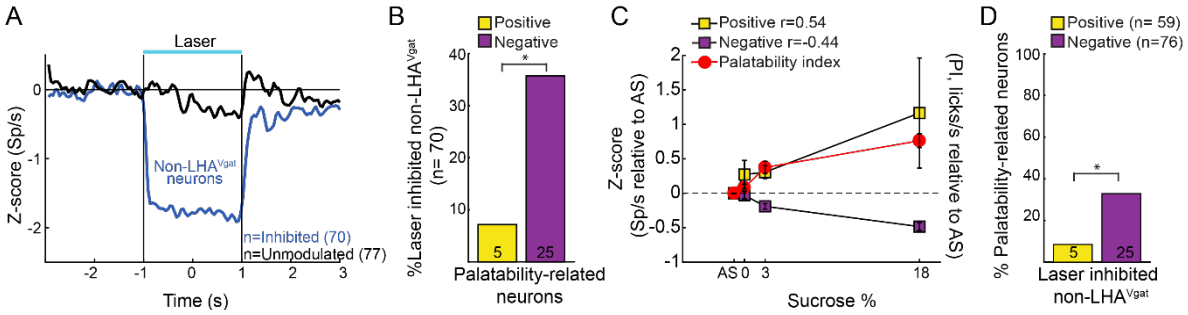

Figure 2— figure supplement 1. Non-LHA^{Vgat} neurons negatively encode sucrose's palatability. (**A**) Responses were aligned to laser onset (Time = 0 s). Relative to baseline (-1 to 0 s) activity, blue and black traces correspond to Inhibited (Non-LHA^{Vgat+} neurons) and Unmodulated responses, respectively. (**B**) Percentage of Non-LHA^{Vgat} neurons whose activity (in the BAT) correlated positively or negatively with the sucrose's PI. * $p < 0.001$, chi-square. (**C**) Z-score activity (relative to AS) for all

Non-LHA^{Vgat} neurons and its correlation with the sucrose's PI. (**D**) Percentage of laser-inhibited non-LHA^{Vgat} with Positive or Negative palatability-related responses. * $p < 0.001$, chi-square.

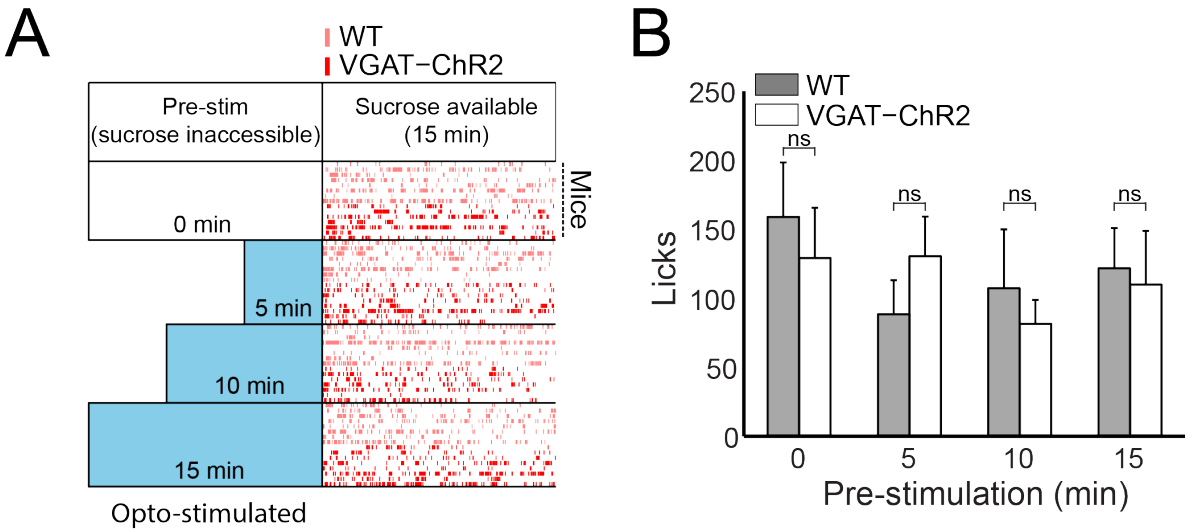

Figure 3— figure supplement 1. Pre-stimulation of LHA^{VGAT+} neurons did not trigger a "hunger state" in that a sustained consummatory behavior is not observed. (**A**) Schematic of the pre-stimulation protocol and raster plot from VGAT-ChR2 (licks were plotted as red ticks) and WT (licks as light red ticks) mice. For this experiment, all mice underwent all pre-stimulation protocols following a Latin square design: 1) mice were pre-stimulated for either 0, 5, 10, or 15 min with no sucrose available. After pre-stimulation, mice received 15 min Free access to a sipper filled with sucrose 10%. (**B**) The average number of licks for sucrose as a function of pre-stimulation. Data were expressed as mean ± SEM.

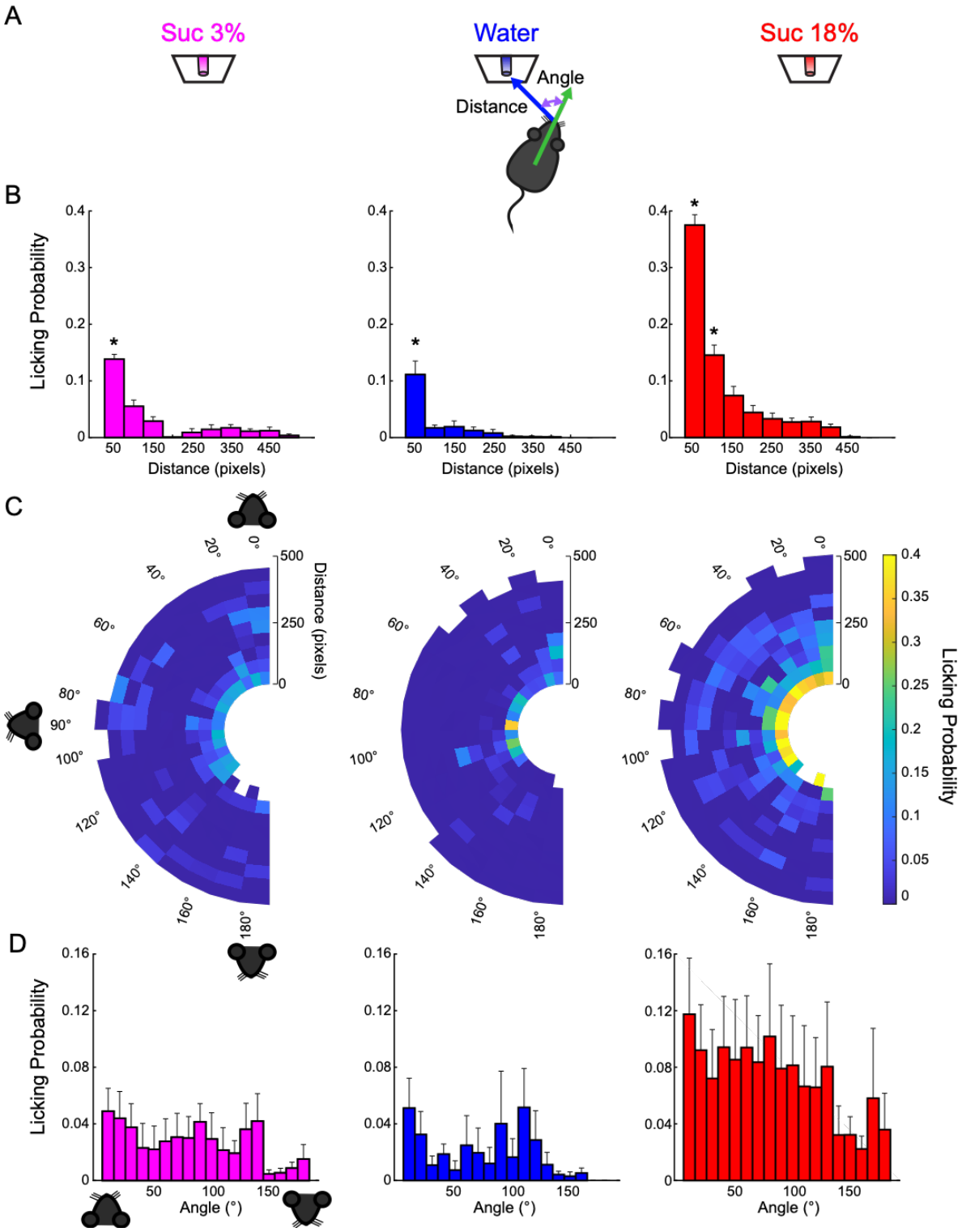

Figure 4— figure supplement 1. Licking probability increased as a function of distance. (**A**) Schematics for video tracking (see Methods). For each laser onset, we calculated the distance and the head angle between the mouse's nose and each of the three sippers containing sucrose 3%, water, or sucrose 18%. (**B**) **It** depicts the probability that laser onset evoked licking as a function of

the mouse's distance relative to each sipper. (**C**) Polar plots are depicting the licking probability after laser onset, given distance and angle of the mouse relative to a licking sipper. At the onset of each laser stimulation, we computed the head angle and distance relative to each sipper, and, in the following 6 s window, we tally if mouse licked to any sipper. We normalized by dividing the number of times licking was elicited by the number of first lasers occurring on those coordinates. The drawing of the mice's head illustrates that if a mouse was facing towards the sipper, the angle is 0°, in perpendicular position (90°), or if it was looking at the opposite direction, the angle was 180°. (**D**) The probability of licking after laser stimulation versus the angle between head direction and the sipper. * Indicates significantly different ($p < 0.001$) relative to all other distances. One-way ANOVA followed by the Holm Sidak test.

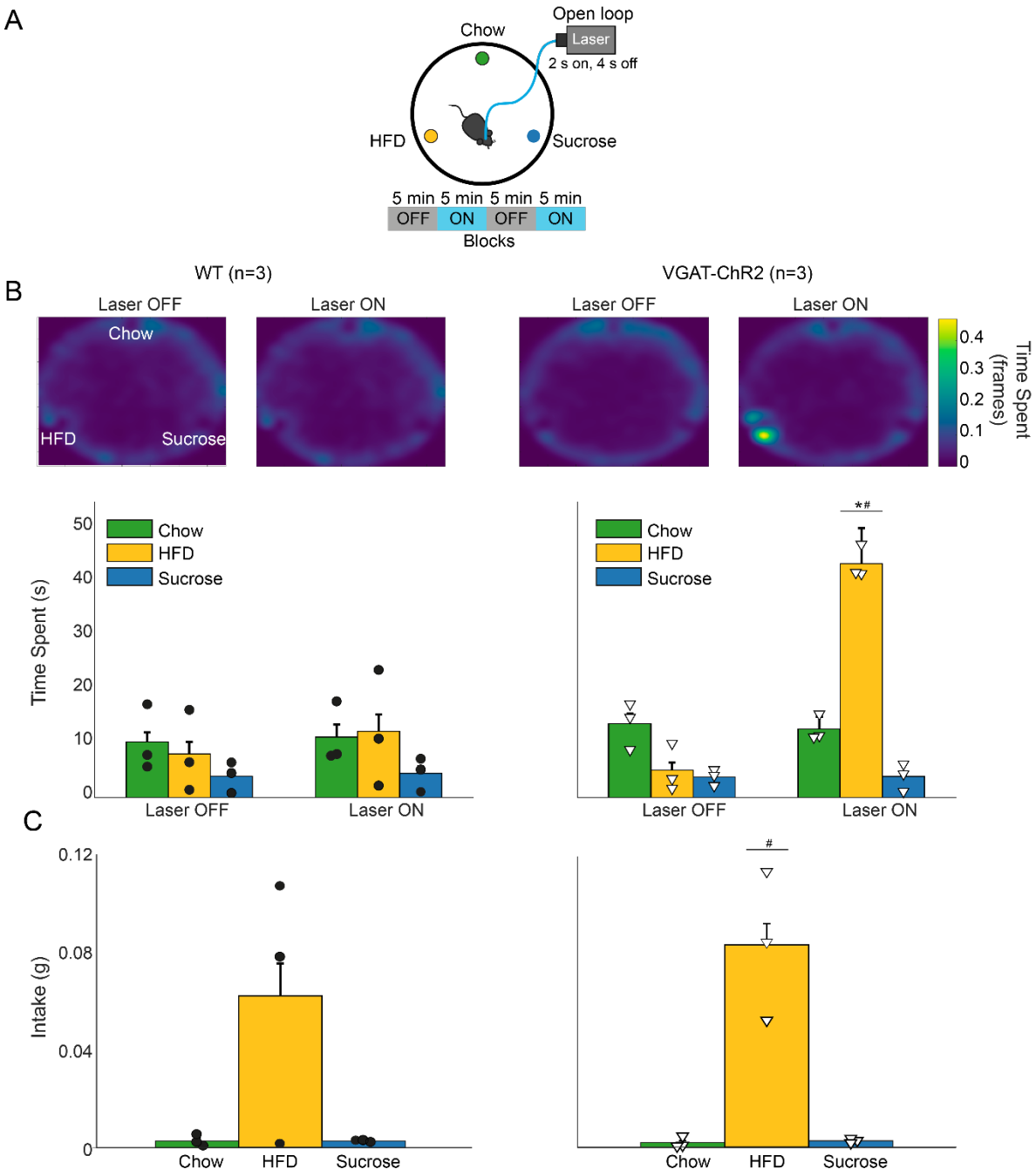

Figure 4— figure supplement 2. Activation of LHA^{Vgat+} neurons increases the time spent near the most palatable High Fat Diet (HFD). (**A**) In a circular arena, three plates containing chow (green), HFD (yellow), and granulated sucrose cube (blue) were available simultaneously. In a 20 min session, the laser was turned "on" following an open loop protocol (2 s on 4 s off during 5 min block with laser and 5 min with no-laser; see Figure 3A). (**B**) Average heat map and time spent in the open field. To create each heat map, we identified the centroid of the mouse at every video frame. Colorbar indicates the number of frames the subject was detected in a given pixel; higher values indicate the mice stayed in that place for a longer time. Time spent (below) was calculated as the distance between the mouse's centroid relative to each food plate. We quantify a food interaction when the subject was within 60 mm distance relative to the plate's center and remained there for at least 1 s. Each dot and triangle represent a single individual. (**C**) Intake of chow, HFD, and granulated sucrose cube. * Denote statistically significant differences ($p < 0.0001$) relative to WT. # $p < 0.0001$ between a stimulus relative to the others. One-way ANOVA followed by the Holm Sidak test. See Video 2.

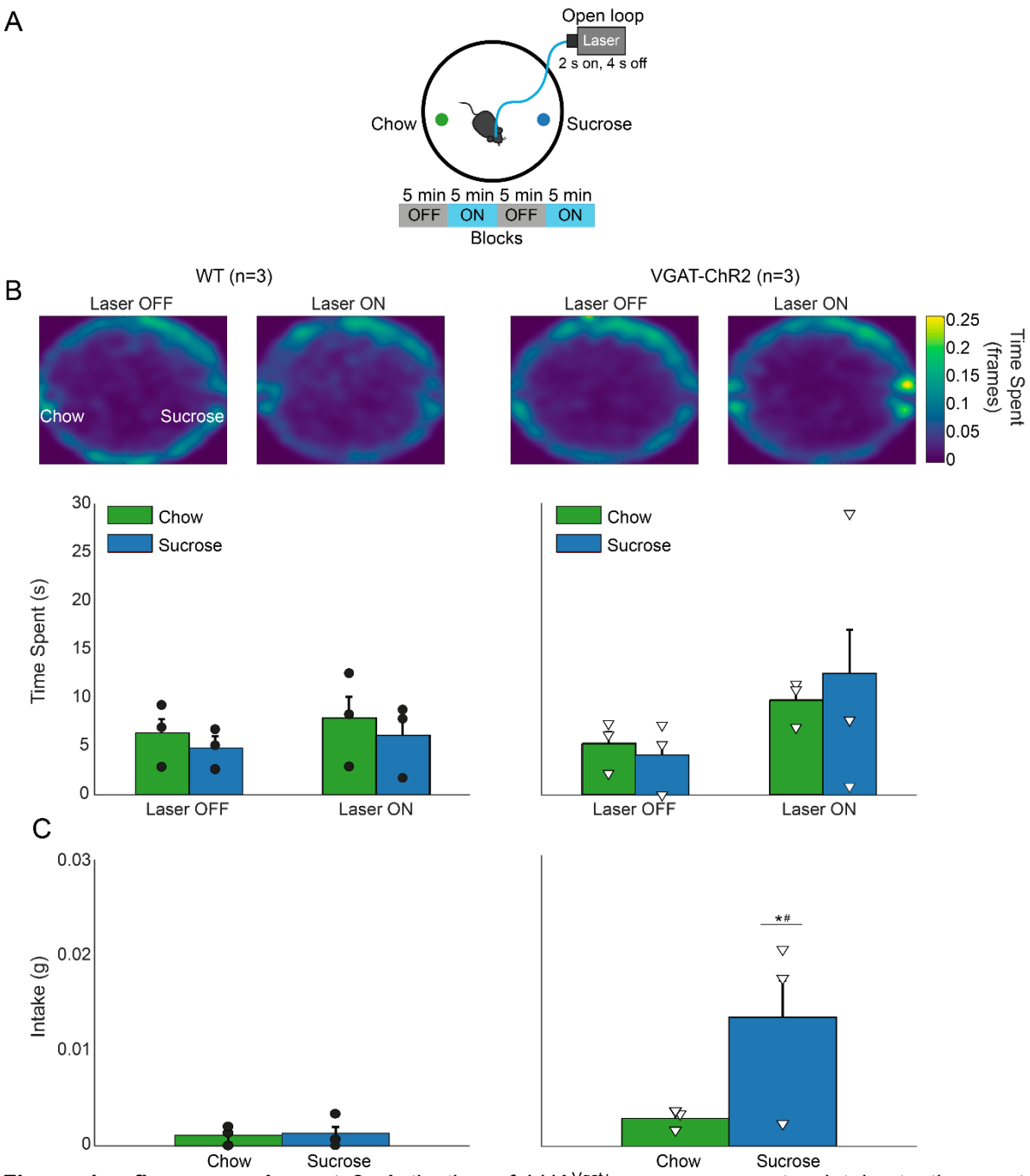

Figure 4— figure supplement 3. Activation of LHA^{Vgat+} neurons promotes intake to the most palatable solid food. (**A**) In a circular arena, Chow pellet and granulated sucrose cube were presented, simultaneously. The laser was turned "on" in an open loop protocol. (**B**) Mean heat map and time spent. The same conventions are in Figure 4— figure supplement 2. (**C**) Intake of chow and granulated sucrose cube. * Statistically significant differences ($p < 0.001$) relative to WT. # $p < 0.0001$ difference between a stimulus relative to the others. One-way ANOVA followed by the Holm Sidak test. See Video 3.

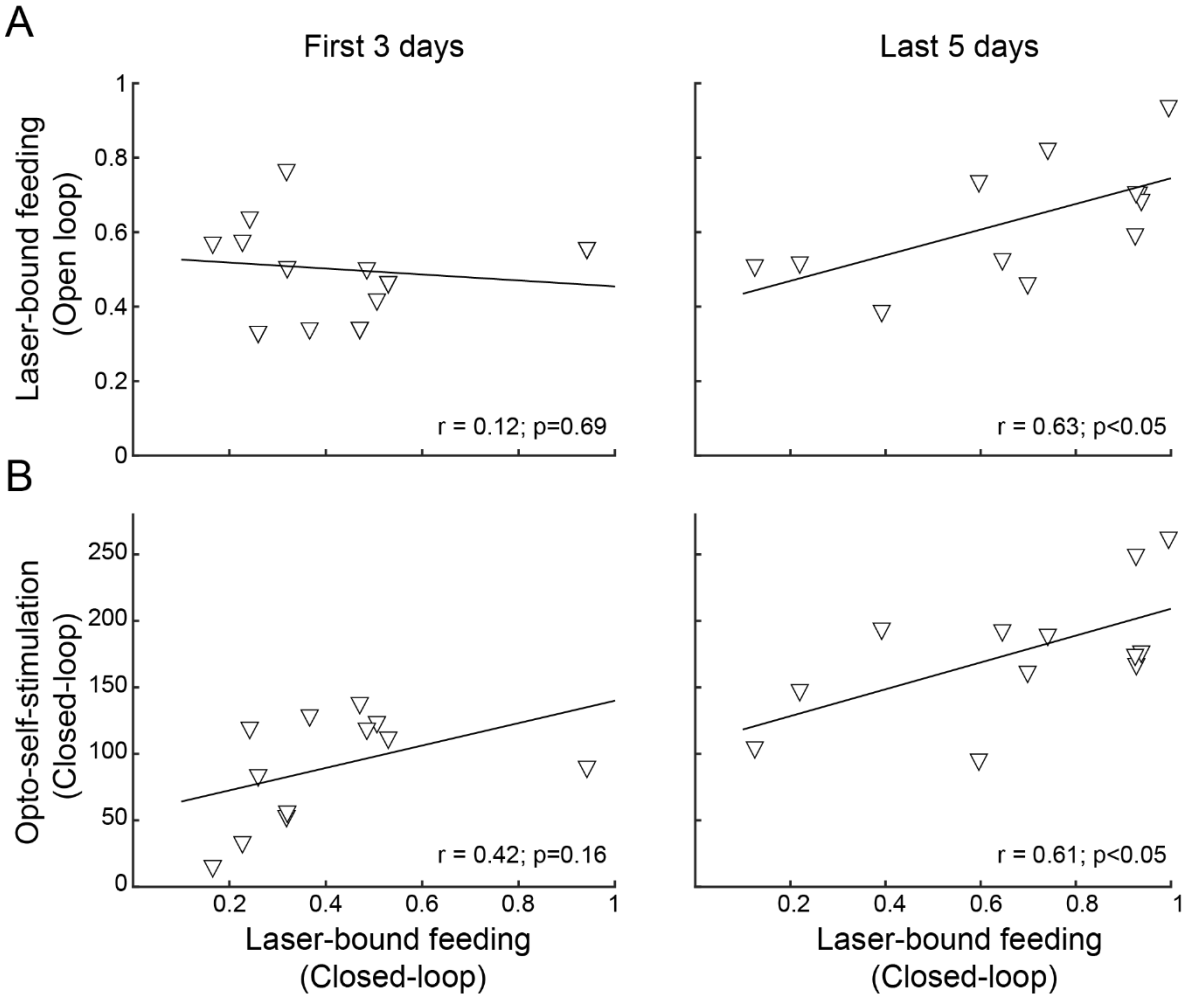

Figure 5— figure supplement 1. After repeated activation of LHA^{Vgat+} neurons, laser-bound feeding (in open vs. closed-loop) strengthened and exhibited a positive correlation. (**A**) Scatter plots showing the relationship between laser-bound feeding (licks given during the 2.5 s window from laser onset relative to total licks in the session) in both open loop and closed-loop tasks during the first 3 days (l*eft panel*) and the last 5 days of opto-stimulation of open loop vs. opto-self-stimulation of the closed-loop protocols (*right panel*). (**B**) Likewise, after repeated activation, both opto-self-stimulations and laser-bound feeding (licking) showed a significant correlation**.** Scatter depicting the average number of opto-self-stimulations vs. the laser-bound feeding observed in the closed-loop protocol.

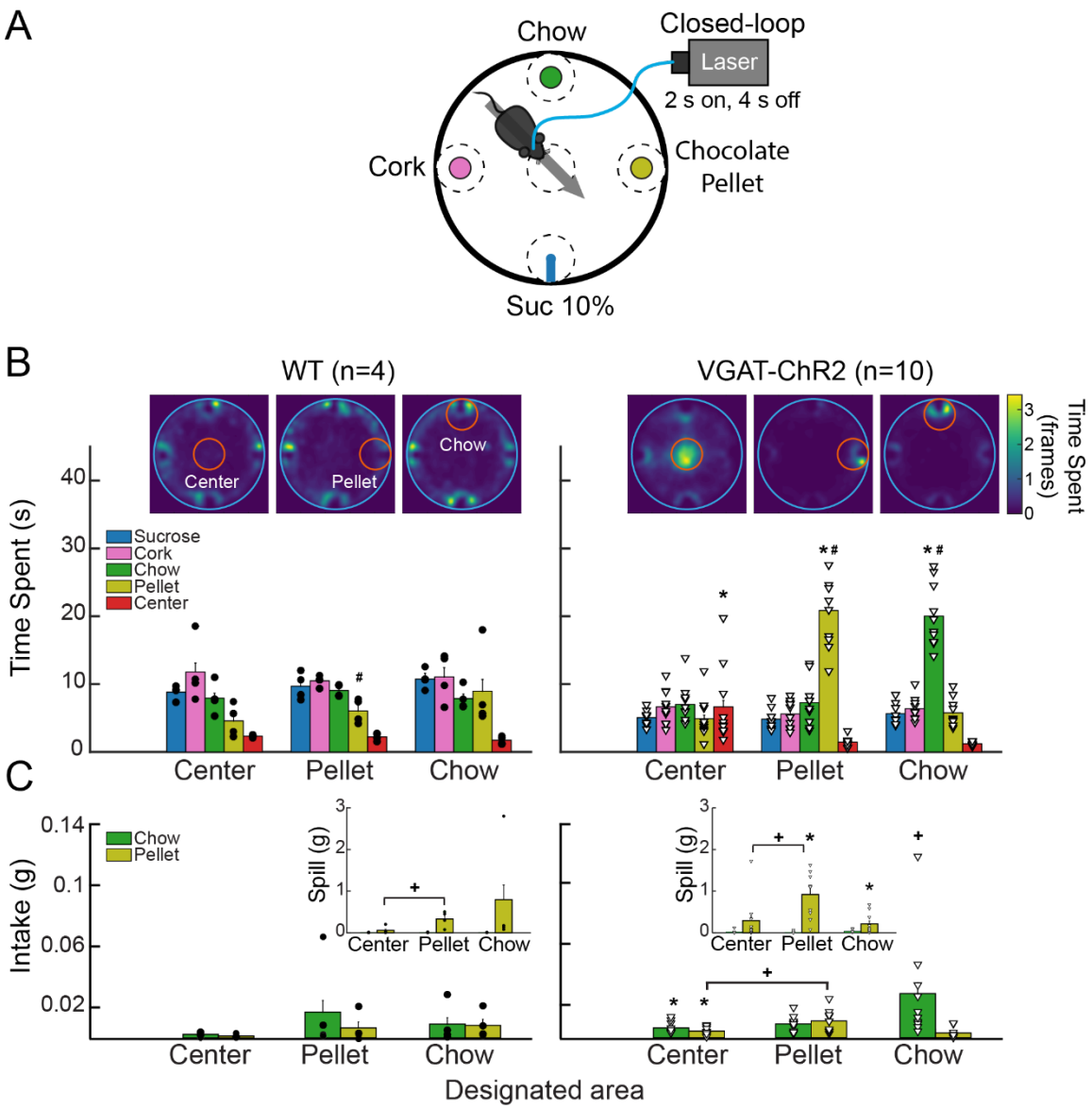

Figure 5— figure supplement 2. Stimulation of LHA^{Vgat+} neurons is rewarding, and biases approach towards the nearest stimulus. (**A**) Different stimuli (plates containing cork, chow, chocolate pellets, or a sipper filled with 10% liquid sucrose) were presented simultaneously in a circular arena. In this task, when mice cross a designated area (dashed circles), the laser was turned on (2 s on; 4 s off) in a 40 min session. Thus, a mouse had to leave and re-enter the designated area to receive a new opto-self-stimulation. Only one designated area was used per session, and it remained in the same position for up to 3 or 4 consecutive days. (**B**) Heat map and time spent from a representative WT (left panel) and VGAT-ChR2 mice (right panels), when the designated area was either the center, the pellet, or the chow (see red circles for the currently designated zone). Colorbar indicates the number of frames the subject was detected in a given pixel; higher values indicate it remained in the same place for a longer time. *Below*, bar graphs depict the time spent in seconds exploring the designated area (within a radius of 5 cm). Each dot and triangle represent a single individual. Though mice normally avoid exploring the center of an open field, opto-self-stimulation in the center zone increased the time transgenic mice spent exploring it, compared with WT. Transgenic mice spent more time exploring the chocolate pellets and the chow food when they were the designated zones. (**C**) Intake of chocolate pellet and chow. Activation of LHA^{Vgat+} neurons in the center zone increased the consumption of both chocolate pellets and chow compared with WT. *Inset*: Spill from chocolate pellets and chow. * Denote

statistically significant differences ($p < 0.05$) relative to WT. + $p < 0.05$ shows a significant increase in consumption and spill during the session that a designated area was opto-self-stimulated relative to the sessions where the center was opto-self-stimulated. Unpaired Student *t*-test. # $p < 0.01$ indicates a significant difference between designated area opto-stimulated and the other areas. One-way ANOVA followed by the Holm Sidak test. See Video 5.

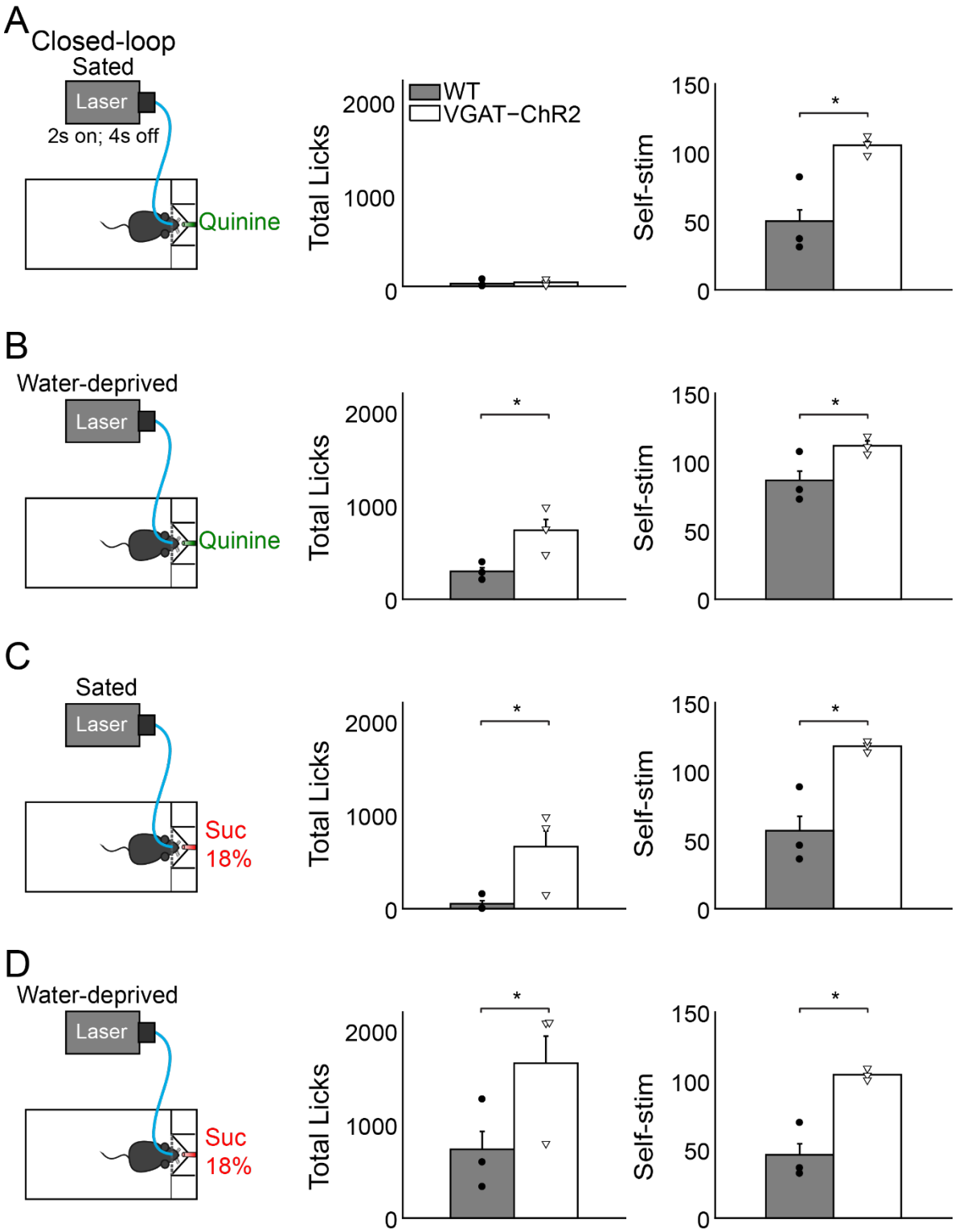

Figure 6— figure supplement 1. Water deprivation gates LHA GABAergic neurons to increase the quinine intake. (**A**) Sated mice had free access to one sipper filled with quinine. The laser was turned on in closed-loop protocol (*left panel*). In sated VGAT-ChR2 mice, activation of these neurons did not increase quinine intake (*central panel*) but continued opto-self-stimulating (*right panel*). (**B**) Water deprived transgenic mice consumed more quinine than in WT mice (*central panel*). (**C-D**) Total licks in the session and number of opto-self-stimulations of 18% sucrose during sated and water deprivation condition. * $p < 0.05$ indicates significant differences compared with WT mice according to an unpaired- t-student test.

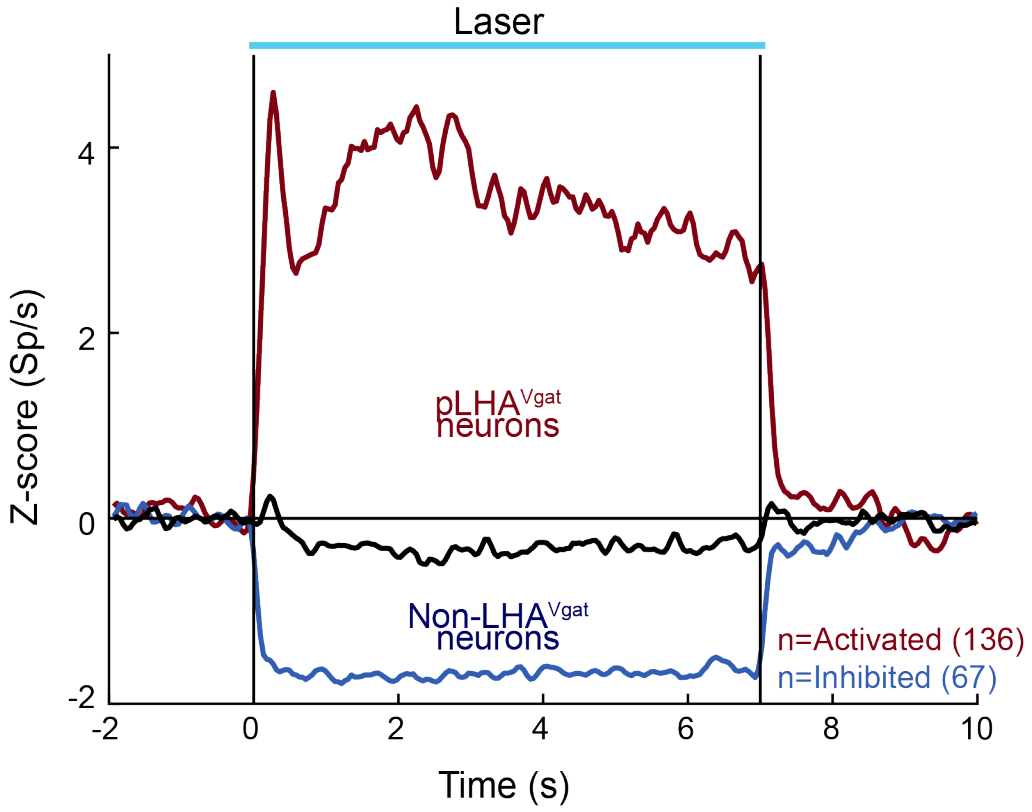

Figure 7— figure supplement 1. Extended opto-stimulation of LHA^{Vgat} neurons evokes responses for up to 7 s. Normalized Z-score population activity of 284 neurons recorded in LHA in VGAT-ChR2 mice (n = 3). The laser was delivered during 7 s at 50 Hz. Neuronal responses were aligned to laser onset (Time = 0 s). Red and blue colors indicate activated or inhibited laser-evoked responses, relative to baseline (-1 to 0 s). Black trace illustrates neurons unmodulated by the laser.

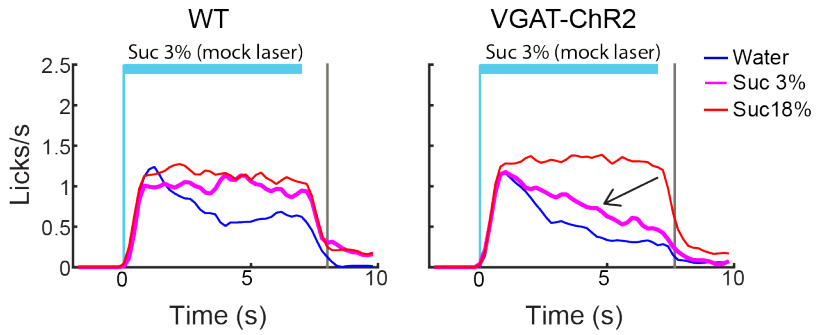

Figure 7— figure supplement 2. Mock laser stimulation did not affect palatability responses. PSTH of licking responses, opto-self-stimulation was delivered along with sucrose 3% trials during 7s (arrow). Mice were connected to a mock optic fiber (with no-laser connected), whereas the real fiber was glued outside the mice's head to emit blue light. Note that both groups increased the lick rate as a function of palatability. The vertical blue line indicates laser onset (Time = 0 s triggered by head entry), whereas the gray line denotes the end of the reward epoch, and the horizontal blue line indicates the photostimulation window.

Video 1. Open loop activation of LHA^{Vgat+} neurons. Water, 3 wt%, and 18 wt% sucrose was delivered in each port. Opto-stimulation occurred in 5 min block of no-laser and 5 min block with the laser.

Video 2. Open loop activation of LHA^{Vgat+} neurons promotes preference toward HFD over granulated sucrose and chow pellet. At equidistant position, three foods were placed on a small plate, and each contained either HFD, chow food, or granulated sucrose cube. Opto-stimulation occurred in 5 min block of no-laser and 5 min block of the laser for 20 min.

Video 3. VGAT-ChR2 mice prefer granulated sucrose over chow food. Preference and intake of granulated sucrose cube vs. chow pellet after open-loop activation of LHA GABAergic neurons.

Video 4. Closed-loop activation of LHA^{Vgat+} neurons. Mice opto-self-stimulate in each head entry in the central licking port (where water is the nearest stimulus). Some VGAT-ChR2 mice exhibited a preference for the most palatable stimulus available (sucrose 18%), whereas others preferred the nearest but less palatable stimulus (water) over sucrose 18%

Video 5. Real-time place preference in an open field task. At equidistant separation, four stimuli were placed on a small plate, and each contained either wood cork, chow pellet, chocolate pellets, or

a sipper a 10% sucrose solution. Mice were photostimulated by 2 s on and 4s off when crossing the designated area.

Video 6. In some VGAT-ChR2 mice, activation of LHA^{Vgat+} neurons induces gnawing to a cork. Wood cork was placed in a transparent box, whereas mice were opto-stimulated in an open loop protocol.